

Migration of *Acanthamoeba* through *Legionella* biofilms is regulated by the bacterial Lqs-LvbR network, effector proteins and the flagellum

Ramon Hochstrasser,¹ Sarah Michaelis,^{1#} Sabrina Brülisauer,^{1#} Thomas Sura,² Mingzhen Fan,¹ Sandra Maaß ,² Dörte Becher² and Hubert Hilbi ^{1*}

¹Institute of Medical Microbiology, University of Zürich, Gloriastrasse 30, Zürich, 8006, Switzerland.

²Institute of Microbiology, University of Greifswald, Felix-Hausdorff-Strasse 8, Greifswald, 17489, Germany.

Summary

The environmental bacterium *Legionella pneumophila* causes the pneumonia Legionnaires' disease. The opportunistic pathogen forms biofilms and employs the lcm/Dot type IV secretion system (T4SS) to replicate in amoebae and macrophages. A regulatory network comprising the *Legionella* quorum sensing (Lqs) system and the transcription factor LvbR controls bacterial motility, virulence and biofilm architecture. Here we show by comparative proteomics that in biofilms formed by the *L. pneumophila* Δ lqsR or Δ lvbR regulatory mutants the abundance of proteins encoded by a genomic 'fitness island', metabolic enzymes, effector proteins and flagellar components (e.g. FlaA) varies. Δ lqsR or Δ flaA mutants form 'patchy' biofilms like the parental strain JR32, while Δ lvbR forms a 'mat-like' biofilm. *Acanthamoeba castellanii* amoebae migrated more slowly through biofilms of *L. pneumophila* lacking lqsR, lvbR, flaA, a functional lcm/Dot T4SS (Δ icmT), or secreted effector proteins. Clusters of bacteria decorated amoebae in JR32, Δ lvbR or Δ icmT biofilms but not in Δ lqsR or Δ flaA biofilms. The amoeba-adherent bacteria induced promoters implicated in motility (P_{flaA}) or virulence (P_{sidC} , P_{ralF}). Taken together, the Lqs-LvbR network (quorum sensing), FlaA (motility) and the lcm/Dot T4SS (virulence) regulate migration of *A. castellanii* through *L. pneumophila* biofilms, and – apart from the T4SS – govern bacterial cluster formation on the amoebae.

Received 4 January, 2022; revised 5 April, 2022; accepted 8 April, 2022. *For correspondence. E-mail hilbi@imm.uzh.ch; Tel. +41 (0) 44 634 2650; Fax +41 (0)44 634 4906. #These authors contributed equally to this work.

Abbreviations

lcm/Dot	intracellular multiplication/defective organelle trafficking;
LAI-1	<i>Legionella</i> autoinducer-1;
LCV	<i>Legionella</i> -containing vacuole;
Lqs	<i>Legionella</i> quorum sensing;
LvbR	<i>Legionella</i> virulence and biofilm regulator;
c-	cyclic di-guanosine monophosphate;
di-GMP	
GFP	green fluorescent protein;
T4SS	type IV secretion system

Introduction

Legionella pneumophila is a Gram-negative environmental bacterium that resides in freshwater niches. Through inhalation of *L. pneumophila*-laden aerosols the opportunistic pathogen reaches the lung and infects alveolar macrophages, which can cause the life-threatening Legionnaires' disease (Fields *et al.*, 2002; Newton *et al.*, 2010; Hilbi *et al.*, 2011). *Legionella pneumophila* replicates intracellularly within free-living protozoa, which appear to represent the preferential niche in the environment (Fields, 1996; Murga *et al.*, 2001; Kuiper *et al.*, 2004). The pathogen governs the interactions with host cells through the lcm/Dot type IV secretion system (T4SS) (Kubori and Nagai, 2016; Ghosal *et al.*, 2019; Böck *et al.*, 2021), which transports the impressive number of >300 different 'effector' proteins implicated in the formation of a unique, ER-associated compartment, the *Legionella*-containing vacuole (LCV) (Isberg *et al.*, 2009; Hubber and Roy, 2010; Finsel and Hilbi, 2015; Personnic *et al.*, 2016; Qiu and Luo, 2017; Steiner *et al.*, 2018).

Legionella pneumophila is a facultative intracellular bacterium, which also colonizes and persists in complex biofilms composed of various microorganisms, including bacteria and protozoa (Lau and Ashbolt, 2009; Declerck, 2010; Abdel-Nour *et al.*, 2013; Hoffmann *et al.*, 2014; Swart *et al.*, 2018). Predatory protozoa, such as the amoeba *Acanthamoeba castellanii*, migrate and 'graze' on the bacterial biofilm communities (Huws *et al.*, 2005). Intriguingly, amoeba migration and endocytic processes such as micropinocytosis are antagonistically correlated, presumably,

since they largely require the same cellular machinery implicated in cytoskeleton and membrane dynamics (Veltman, 2015; Delgado *et al.*, 2022). Intracellular replication within amoebae seems to promote bacterial features that facilitate biofilm formation by *L. pneumophila* (Bigot *et al.*, 2013) and is likely important for *L. pneumophila* to grow within multispecies biofilms (Declerck *et al.*, 2007; Declerck *et al.*, 2009).

Under laboratory conditions, *L. pneumophila* forms mono-species biofilms that allow the investigation of bacterial determinants potentially implicated in biofilm development (Mampel *et al.*, 2006; Hindré *et al.*, 2008; Pécastaings *et al.*, 2010; Hochstrasser *et al.*, 2019). *Legionella pneumophila* biofilm formation is not well understood, and only a few bacterial determinants affecting biofilm formation have been described (Abu Khweik and Amer, 2018). The Tat transporter (De Buck *et al.*, 2005), the *Legionella* collagen-like (Lcl) adhesin (Duncan *et al.*, 2011; Mallegol *et al.*, 2012) and to a limited extent the type IV pili (Lucas *et al.*, 2006) have been found to be involved in biofilm development.

The flagellum assists biofilm development of various bacteria (Davey and O'Toole, 2000; Petrova and Sauer, 2012). The *L. pneumophila* flagellum filament protein (flagellin) is encoded by the *flaA* gene, and its transcription is controlled by the alternative sigma factor FliA (Albert-Weissenberger *et al.*, 2010). The production of sessile *L. pneumophila* biomass is regulated by FliA and seems to be independent of FlaA (Mampel *et al.*, 2006;

Stewart *et al.*, 2012), but it remains unclear to which extent FlaA mediates the *L. pneumophila* biofilm architecture.

The pleiotropic transcription factor LvbR (*Legionella* virulence and biofilm regulator) controls *L. pneumophila* virulence and biofilm architecture, and its transcription is negatively regulated by the *Legionella* quorum sensing (Lqs) kinase LqsS (Hochstrasser *et al.*, 2019; Hochstrasser and Hilbi, 2020) (Fig. 1). LvbR negatively regulates the nitric oxide (NO) sensor and di-guanylate cyclase inhibitor Hnox1, and thus, positively regulates the production of the second messenger cyclic di-guanosine monophosphate (c-di-GMP). Several c-di-GMP metabolizing enzymes are implicated in the regulation of *L. pneumophila* biofilm formation (Carlson *et al.*, 2010; Pécastaings *et al.*, 2016).

The Lqs system comprises the autoinducer synthase LqsA (Spirig *et al.*, 2008), the sensor histidine kinases LqsS (Tiaden *et al.*, 2010b) and LqsT (Kessler *et al.*, 2013), and the response regulator LqsR (Tiaden *et al.*, 2007; Tiaden *et al.*, 2008), which dimerizes upon phosphorylation (Schell *et al.*, 2014; Hochstrasser *et al.*, 2020). The Lqs system produces, detects and responds to the signalling molecule LAI-1 (*Legionella* autoinducer-1, 3-hydroxypentadecane-4-one) (Tiaden *et al.*, 2010a; Tiaden and Hilbi, 2012). The system regulates various traits in *L. pneumophila* (Fig. 1), such as motility and production of flagellin (Schell *et al.*, 2016), virulence (Hochstrasser and Hilbi, 2017; Personnic *et al.*, 2018), the bacterial growth phase switch (Tiaden *et al.*, 2007; Hochstrasser and Hilbi, 2022), expression of

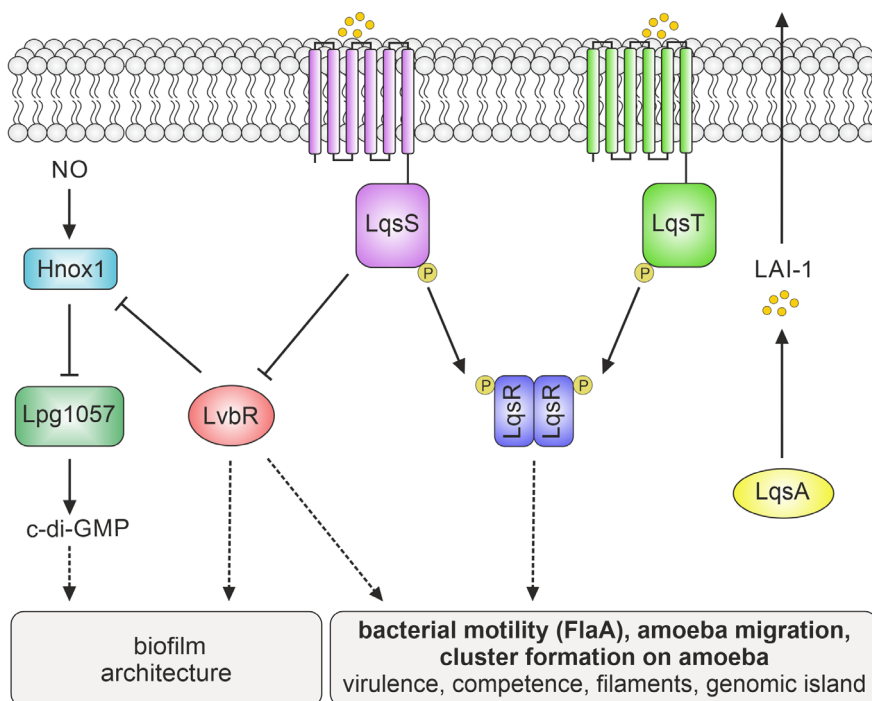


Fig. 1. The *L. pneumophila* Lqs-LvbR regulatory network. The Lqs (*Legionella* quorum sensing) system produces, detects and responds to the small signalling molecule LAI-1 (*Legionella* autoinducer-1, 3-hydroxypentadecane-4-one). The system comprises the autoinducer synthase LqsA, the cognate membrane-bound sensor kinases LqsS and LqsT, and the prototypic response regulator LqsR. LqsS negatively regulates the expression of *lvbR*, encoding the transcription factor LvbR (*Legionella* virulence and biofilm regulator). In turn, LvbR negatively regulates the expression of *hnox1*, encoding the NO sensor Hnox1, to control the diguanylate cyclase Lpg1057, c-di-GMP levels and biofilm architecture. The Lqs-LvbR network regulates bacterial growth phase switch and motility (flagellin, FlaA), amoeba migration in biofilms and bacterial cluster formation on amoebae, virulence, competence and extracellular filaments, as well as the expression of genes on a 133 kb genomic island, including *lvbR*.

a genomic ‘fitness island’ and natural competence for DNA uptake (Hochstrasser and Hilbi, 2017; Personnic *et al.*, 2018), as well as host cell motility (Simon *et al.*, 2015). However, it is not known to what extent the Lqs system controls biofilm formation or architecture.

The interactions between biofilm/sessile bacterial pathogens and amoebae represent crucial ecological processes, which are not well understood on a molecular level. It is currently not known to which extent bacterial factors, such as regulatory systems, virulence factors, the flagellum, or the architecture of biofilms determine the encounter with amoebae. In this study, we visualized and quantified by confocal microscopy the interactions of amoebae with genetically distinct *L. pneumophila* biofilms. We found that the Lqs regulator LqsR, the transcription factor LvbR, the flagellum and the Icm/Dot T4SS control the migration of *A. castellanii* through *L. pneumophila* biofilms, and – with the exception of the T4SS – also regulate bacterial adherence and cluster formation on the amoeba surface.

Results

Comparative proteomics and differential regulation of flagellum production in *L. pneumophila* $\Delta lvbR$ or $\Delta lqsR$ biofilms

The *L. pneumophila* transcription factor LvbR regulates biofilm architecture: biofilms formed by a $\Delta lvbR$ mutant are homogenous and ‘mat-like’, while biofilms formed by the parental strain JR32 appear aggregated and ‘patchy’ respectively (Hochstrasser *et al.*, 2019). To further identify components relevant for *L. pneumophila* biofilm formation, we compared the proteomes of biofilms formed by JR32, $\Delta lvbR$ or $\Delta lqsR$ mutant strains. To this end, the strains were left to form biofilms in AYE medium for 6 days, bacteria-associated and secreted proteins were collected, and the proteomes of the mutant strains were compared to the parental strain JR32 (Fig. 2A, Fig. S1). In biofilms formed by the $\Delta lvbR$ strain, there were ca. 1.7 times more proteins produced than that in biofilms formed by the $\Delta lqsR$ strain (Fig. 2A). Among a total of 1241 proteins identified, 662 or 237 were uniquely produced in $\Delta lvbR$ or $\Delta lqsR$ biofilms respectively, while 342 were produced in concert in biofilms from both strains, the abundance of which changed synergistically (326 proteins) or reciprocally (16 proteins). Hence, in biofilms formed by the $\Delta lvbR$ or $\Delta lqsR$ mutants significantly more protein abundances changed jointly rather than reciprocally (Fig. 2A, Fig. S1). These results suggest that the regulators LvbR and LqsR share many common targets in biofilms.

A number of proteins with substantially changed abundances were identified in biofilms formed by the $\Delta lvbR$ or $\Delta lqsR$ mutant strains (Fig. S1). Specifically, proteins produced by the 133 kb genomic fitness island region I

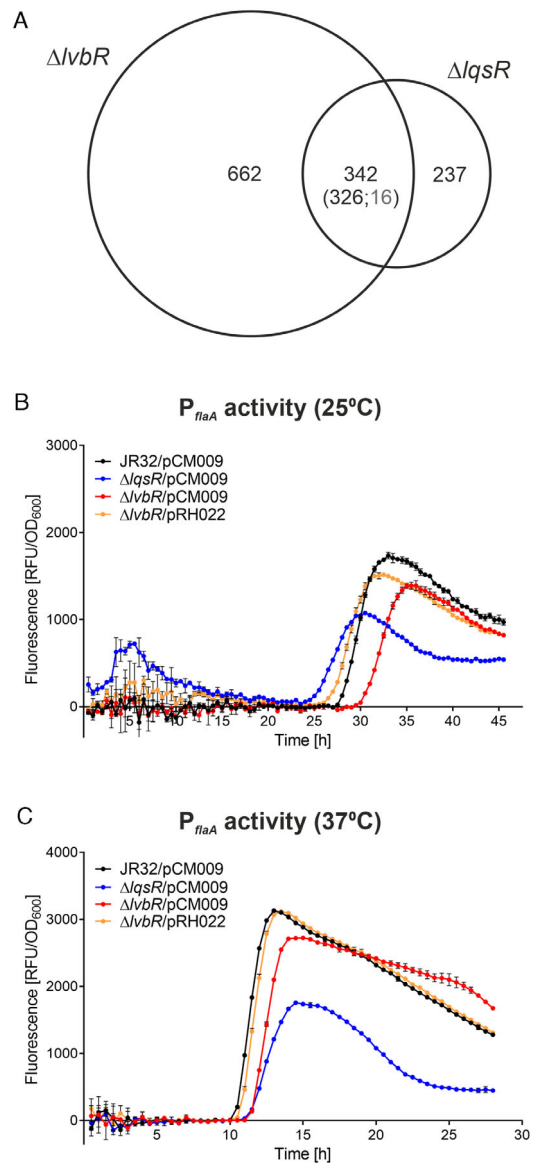


Fig. 2. Comparative proteomics of *L. pneumophila* JR32, $\Delta lvbR$ and $\Delta lqsR$ biofilms and validation of differential P_{flaA} expression.

A. Proteomics was performed with biofilms formed by $\Delta lvbR$ or $\Delta lqsR$ mutant strains and compared to the biofilms formed by the parental strain JR32. In the Venn diagrams all proteins are shown that are depleted or enriched in mutant biofilms (for details see Materials and Methods). Among the total of 1241 proteins identified, 342 were produced in concert depending on the presence of LvbR and LqsR (overlapping area; brackets: number of LvbR/LqsR-dependent proteins, which accumulate in parallel (326, black) or reciprocally (16, grey)).

B, C. P_{flaA} -gfp expression in $\Delta lvbR$ and $\Delta lqsR$ mutant strains. *Legionella pneumophila* JR32, $\Delta lvbR$ or $\Delta lqsR$ strains harbouring the promoter-reporter constructs P_{flaA} -gfp (pCM009) or $P_{lvbR-lvbR}$ -gfp (pRH022) were grown at (B) 25°C or (C) 37°C in AYE medium within microplates while orbitally shaking. GFP fluorescence (relative fluorescence units, RFU) at a gain of 50 and optical density at 600 nm (OD_{600}) were measured over time using a microplate reader. The kinetics of the GFP fluorescence/ OD_{600} values are shown. The data are means and standard deviations of a technical triplicate and representative of two (B) or three (C) independent measurements.

(*lpg0973-lpg1005*; e.g. Lpg0987, Lpg0995) and region II (*lpg1006-lpg1096*; e.g. Lpg1055) were less (region I) or more (region II) abundant in biofilms formed by the mutant strains (Fig. S1, box 1–2). Moreover, the *Legionella* collagen-like (Lcl) adhesin (Lpg2644; SclB tail fibre protein) (Duncan *et al.*, 2011; Mallegol *et al.*, 2012) was found in lower amounts in the $\Delta lvbR$ mutants compared to the wild-type strain (Fig. S1). Components of the Lvh T4SS (LvhB5/Lpg1253, LvhB10/Lpg1247, LvrE/Lpg1244) (Segal *et al.*, 1999) (Fig. S1, box 3) and lcm/Dot-translocated effector proteins, such as the astacin protease LegP (Lpg2999) (de Felipe *et al.*, 2008), the deAMPylase SidD (Lpg2465) (Neunuebel *et al.*, 2011; Tan and Luo, 2011), the ubiquitin ligase SdeA (Lpg2157) (Qiu *et al.*, 2016), the Rab1 GEF RalF (Lpg1950) (Nagai *et al.*, 2002) and the protein kinase Lpg2603 (Sreelatha *et al.*, 2020) were found in lower amounts in the $\Delta lvbR$ and/or $\Delta lqsR$ mutants compared to the parental strain JR32 (Fig. S1). In contrast, enzymes implicated in *myo*-inositol catabolism, such as lolG (Lpg1652), lolCB (Lpg1651), lolD (Lpg1650) and lolE (Lpg1649) (Manske *et al.*, 2016) were more abundant in biofilms formed by the $\Delta lvbR$ or $\Delta lqsR$ mutant strains (Fig. S1, box 4), indicating that inositol catabolism in *L. pneumophila* biofilms might be negatively regulated by LvbR and LqsR.

Intriguingly, in biofilms formed by the $\Delta lvbR$ or $\Delta lqsR$ mutant strains components of the flagellum were differentially produced, in particular the major flagellar subunit flagellin (FlaA/FliC, Lpg1340) was depleted, while the flagellar hook-associated protein FliD (Lpg1338), some Flg proteins (Lpg1218–Lpg1222), the flagellar motor switch protein FliN (Lpg1791) and other Fli proteins (Lpg1758, Lpg1762), as well as the flagellar biosynthesis sigma factor FliA (Lpg1782) were enriched (Fig. S1, box 5–8).

In agreement with these findings, in the $\Delta lvbR$ and $\Delta lqsR$ mutant strains the expression of a P_{flaA} -*gfp* reporter construct lagged behind and was downregulated at 25°C (Fig. 2B) as well as at 37°C (Fig. 2C), confirming previous results for $\Delta lqsR$ (Schell *et al.*, 2016). Complementation of the $\Delta lvbR$ mutant phenotype was achieved with a plasmid producing LvbR under control of its natural promoter (P_{lvbR} -*lvbR*) in addition to GFP under control of P_{flaA} (Fig. 2B and C). In agreement with the finding that components of the flagellum are downregulated in the $\Delta lvbR$ and $\Delta lqsR$ strains, the mutants showed reduced motility upon growth in AYE medium (Movies S1–S3). Taken together, these results suggest that LqsR and LvbR control the production of the flagellum, and in particular, act as positive regulators of FlaA production and *flaA* transcription.

Based on the finding that the flagellum is regulated by LqsR and LvbR in *L. pneumophila* biofilms, we assessed whether FlaA is a determinant of biofilm formation and architecture. To this end, GFP-producing *L. pneumophila* JR32 or $\Delta flaA$ were left to form biofilms in AYE medium for 1, 2, 3 and 6 days at 25°C without disturbance, and

biofilm formation, including architecture and adherence to an abiotic surface, was analysed by confocal microscopy (Fig. 3). Under these conditions, the $\Delta flaA$ mutant strain showed the same ‘clustered’ and ‘patchy’ biofilm architecture as the parental JR32 strain. In contrast, the $\Delta lvbR$ strain formed a ‘mat-like’ biofilm, as reported previously (Hochstrasser *et al.*, 2019).

Analogously, we assessed the *L. pneumophila* $\Delta lqsR$, $\Delta lqsA$, $\Delta lqsS$, $\Delta lqsT$ and $\Delta lqsS$ - $\Delta lqsT$ mutant strains for biofilm formation. The *lqs* mutant strains formed biofilms with the same morphology as the parental strain JR32 (Fig. 3, Fig. S2A), produced comparable biomass, i.e. the same number of bacteria per ml (Fig. S2B and C), and adhered similarly to the abiotic surface of the microscopy dish (Fig. S3). In summary, biofilms formed by *L. pneumophila* lacking the major flagellum component FlaA or components of the Lqs system adopt a ‘patchy’ architecture morphologically similar to the parental strain JR32, produce a comparable biomass, and adhere indistinguishably to an abiotic surface. Therefore, under the conditions tested the flagellum is not required to establish *L. pneumophila* biofilms, and quorum sensing does not control biofilm formation and architecture. However, since the biofilms formed by the $\Delta lvbR$ or $\Delta lqsR$ mutants regulate flagellum production and differ in their protein pattern compared to JR32 (Fig. S1), a distinct protein composition underlies these morphologically similar biofilms.

LvbR, *LqsR* and *FlaA* promote *A. castellanii* migration through *L. pneumophila* biofilms

To further investigate the characteristics of genetically different *L. pneumophila* biofilms, we assessed their interactions with amoebae. The different protein composition profiles of biofilms formed by *L. pneumophila* JR32 or mutant strains might affect the migration of amoebae through a biofilm. To test this hypothesis, we quantified the migration of *A. castellanii* through biofilms formed by GFP-producing *L. pneumophila* JR32 or the $\Delta lvbR$, $\Delta lqsR$, $\Delta lqsA$ or $\Delta flaA$ mutant strains (Fig. 4). The biofilms were grown in AYE medium for 6 days at 25°C, and after adding the amoebae, the migration of single cells through the biofilms was tracked by confocal microscopy in the bright field channel (Movies S4–S8).

Under these conditions, the amoebae within JR32 or $\Delta lqsA$ biofilms showed a more vigorous migration compared to $\Delta lvbR$, $\Delta lqsR$ or $\Delta flaA$ biofilms (Fig. 4A). The amoebae velocity was highest in biofilms formed by JR32 (on average ca. 0.22 $\mu\text{m s}^{-1}$), lower in biofilms generated by $\Delta lvbR$ or $\Delta flaA$ (ca. 0.15 $\mu\text{m s}^{-1}$, not significant for $\Delta lqsA$) and lowest in $\Delta lqsR$ biofilms (ca. 0.09 $\mu\text{m s}^{-1}$) (Fig. 4B). The migration distance (Euclidean distance) was ca. 75 μm for amoebae in biofilms formed by JR32,

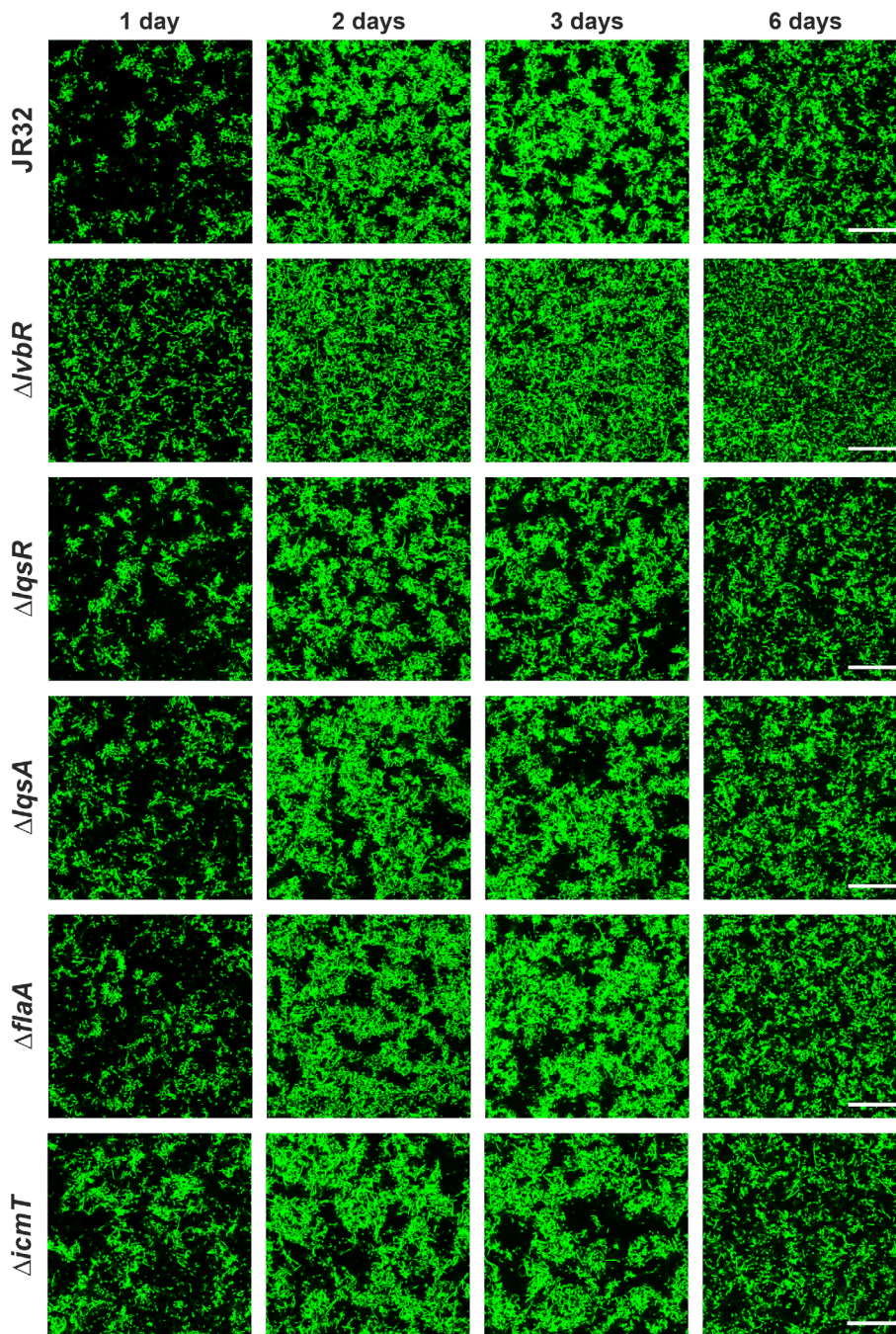


Fig. 3. Biofilm formation of *L. pneumophila* Δlqs , $\Delta flaA$ and $\Delta icmT$ mutant strains. Biofilms were initiated with exponential phase *L. pneumophila* JR32, $\Delta lvsR$, $\Delta lqsR$, $\Delta lqsA$, $\Delta flaA$ or $\Delta icmT$ mutant strains harbouring pNT28 (constitutive production of GFP) in AYE medium within ibiTreat microscopy dishes. Biofilms were grown at 25°C without mechanical disturbance, and confocal microscopy images of biofilm architecture were acquired at 4 μm above the dish bottom after 1, 2, 3 and 6 days of growth. The images shown are representative of three independent experiments. Scale bars, 30 μm .

$\Delta lqsA$ or $\Delta flaA$ and less (but not significantly) for amoebae in biofilms formed by the $\Delta lvsR$ or $\Delta lqsR$ mutant strains (ca. 40 μm) (Fig. 4C). These observations were rather unexpected, since the JR32 and $\Delta lqsA$ strains are more virulent (and thus potentially more toxic) than the $\Delta lvsR$, $\Delta lqsR$ or $\Delta flaA$ mutant strains. Taken together, *A. castellanii* amoebae migrate fastest in biofilms established by *L. pneumophila* JR32, with intermediate speed in $\Delta lqsA$, $\Delta flaA$ or $\Delta lvsR$ biofilms and slowest in biofilms formed by $\Delta lqsR$. Thus, amoeba migration in *L.*

pneumophila biofilms is positively correlated to the virulence of a strain and promoted by LqsR and LvsR as well as by FlaA.

The Icm/Dot T4SS and the effector LegG1 promote A. castellanii migration through L. pneumophila biofilms

Given the positive correlation between amoeba migration and the *L. pneumophila* virulence regulators LqsR and

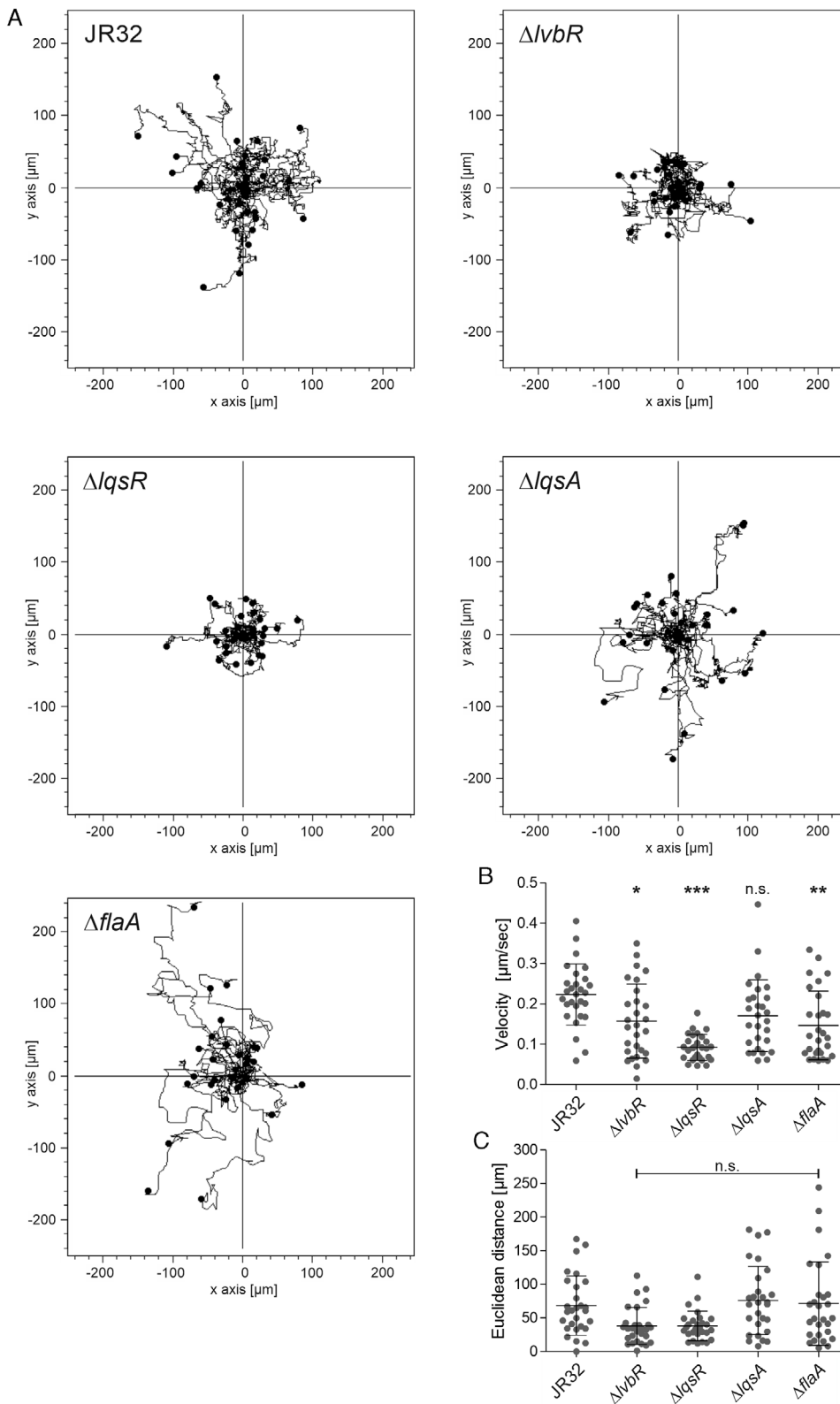


Fig. 4. LvbR, LqsR and FlaA promote *A. castellanii* migration through *L. pneumophila* biofilms. Biofilms of *L. pneumophila* JR32, $\Delta lvbR$, $\Delta lqsR$, $\Delta lqsA$ or $\Delta flaA$ mutant strains harbouring pNT28 (constitutive production of GFP) were grown in AYE medium at 25°C. *A. castellanii* was added to preformed biofilms after 6 days, and amoeba migration was followed by confocal microscopy.

A. Single amoeba migrating through biofilms were tracked and individually shown as a line in migration plots.

B. The velocities and (C) Euclidean distances of migrating amoebae tracked in (A) were quantified. The data (B, C) are means and standard deviations of the mean derived from all tracked amoebae (n.s., not significant; * $p \leq 0.05$; ** $p \leq 0.01$; *** $p \leq 0.001$; one-way ANOVA with Tukey post-test; JR32 vs. mutant strains). Single amoebae were tracked in three biologically independent experiments with a total of $n = 28$ amoebae for each bacterial strain.

LvbR (Fig. 4), we next tested the role of the Icm/Dot T4SS and secreted effector proteins for amoeba migration in *L. pneumophila* biofilms. To this end, we used the

$\Delta icmT$ mutant strain, which lacks a functional Icm/Dot T4SS (Böck *et al.*, 2021), is defective for intracellular growth (Segal and Shuman, 1998), and in contrast to the

wild-type strain JR32, does not inhibit cell migration upon infection (Simon *et al.*, 2014). Moreover, we used the ΔlegG1 (*lpg1976*), ΔppgA (*lpg2224*) or $\Delta\text{legG1-}\Delta\text{ppgA}$ mutant strains, lacking one or two RCC1 repeat effectors, which promote microtubule stabilization, LCV motility and host cell migration (Rothmeier *et al.*, 2013; Swart *et al.*, 2020b). Biofilms formed by the ΔicmT mutant strain in AYE medium for 1, 2, 3 and 6 days at 25°C without disturbance were morphologically similar to the parental strain JR32 (Fig. 3), and the mutant adhered similarly (but due to faster growth more densely) to an abiotic surface (Fig. S3). Therefore, a functional lcm/Dot T4SS is not required for normal *L. pneumophila* biofilm formation.

We compared the migration of *A. castellanii* through biofilms formed by *L. pneumophila* JR32, or the ΔicmT , ΔlegG1 , ΔppgA or $\Delta\text{legG1-}\Delta\text{ppgA}$ mutant strains (Fig. 5). To this end, the biofilms were grown in AYE medium for 6 days at 25°C, and after adding the amoebae, the migration of single cells through the biofilms was tracked by confocal microscopy in the bright field channel (Movies S4 and S9). In JR32 biofilms the amoebae showed a more vigorous migration compared to biofilms established either by the ΔicmT , ΔlegG1 , ΔppgA or the $\Delta\text{legG1-}\Delta\text{ppgA}$ double mutant strain (Fig. 5A). The amoeba velocity was highest in biofilms formed by JR32 (on average ca. $0.3 \mu\text{m s}^{-1}$), followed by ΔppgA (ca. $0.28 \mu\text{m s}^{-1}$), and significantly lower in ΔlegG1 or $\Delta\text{legG1-}\Delta\text{ppgA}$ biofilms (ca. $0.15\text{--}0.16 \mu\text{m s}^{-1}$). Interestingly, amoeba movement was most strongly impaired in ΔicmT biofilms (ca. $0.09 \mu\text{m s}^{-1}$) (Fig. 5B). The migration distance (Euclidean distance) was highest for amoebae in biofilms formed by JR32 (ca. $90 \mu\text{m}$), lowest in biofilms formed by ΔicmT (ca. $40 \mu\text{m}$) and intermediate for amoebae in biofilms formed by the ΔlegG1 , ΔppgA or $\Delta\text{legG1-}\Delta\text{ppgA}$ mutant strains (ca. $60\text{--}70 \mu\text{m}$) (Fig. 5C).

In summary, compared to biofilms formed by the parental strain JR32, *A. castellanii* amoebae migrate less vigorously in biofilms formed by mutant strains lacking a functional lcm/Dot T4SS or RCC1 repeat effectors. Amoeba movement was most strongly impaired in ΔicmT biofilms, suggesting that in addition to the RCC1 repeat effectors other lcm/Dot substrates might also contribute to promoting protozoan motility. Hence, amoeba migration in *L. pneumophila* biofilms is positively correlated to the lcm/Dot-dependent virulence, similar to what was observed for biofilms formed by regulatory (and *flaA*) mutant strains (Fig. 4).

LvbR, *LqsR* and *FlaA* determine *L. pneumophila* cluster formation on *A. castellanii*

To further investigate the processes underlying the migration of *A. castellanii* through biofilms, we analysed by confocal microscopy the features of different *L.*

pneumophila strains interacting with the amoebae. To this end, GFP-producing *L. pneumophila* JR32 or the ΔlvbR , ΔlqsR , ΔlqsA , ΔflaA or ΔicmT mutant strains were left to form biofilms in AYE medium for 6 days at 25°C, and bacteria–amoeba interactions were assessed by confocal microscopy in the GFP or bright field channel respectively (Fig. 6).

Strikingly, amoebae placed onto biofilms generated by JR32, ΔlqsA or ΔicmT were decorated with bacteria that formed large aggregates or clusters adhering to the amoebae (Fig. 6A). Close-up inspection (Fig. S4A) and 3D-rendering (Fig. S4B) of these bacterial aggregates revealed multi-layered clusters decorating the polar or lateral side of amoebae, and preferentially the lagging end of moving amoebae (Movies S4 and S7). Furthermore, ‘trails’ of migrating amoebae were apparent in the surface-attached layer of JR32 biofilms, suggesting that the migrating amoebae ‘grazed’ through biofilms leaving behind a track devoid of bacteria (Fig. S4C, Movies S4 and S7).

The quantitative assessment of the clusters by confocal microscopy revealed that almost 100% of the amoebae in biofilms formed by the JR32, ΔlqsA , or ΔicmT strains were decorated by bacterial clusters (Fig. 6B). In contrast, ca. 75% of the amoebae were decorated with bacterial clusters in biofilms formed by the ΔlvbR strain, and only ca. 10% of the amoebae were decorated with bacterial clusters in biofilms formed by the ΔlqsR or ΔflaA mutant strains. Moreover, the size of the bacterial clusters was similar for strain JR32, ΔlqsA or ΔicmT (ca. $30 \mu\text{m}^2$), and significantly smaller for the ΔlvbR , ΔlqsR or ΔflaA mutant strains (ca. $10\text{--}20 \mu\text{m}^2$) (Fig. 6C). The quantification of the clusters by flow cytometry indicated very similar results: the amoeba-associated fluorescence intensity of GFP-producing *L. pneumophila* was highest for the JR32, ΔlqsA , or ΔicmT strains, followed by ΔlvbR , and lowest for the ΔlqsR or ΔflaA mutant strains (Fig. 6D, Fig. S5AB). In summary, these observations indicate that *L. pneumophila* forms large aggregates or clusters adhering to amoebae within biofilms, and neither the LqsA-produced quorum-sensing signalling molecule LAI-1 nor the lcm/Dot T4SS are required for cluster formation.

In contrast to the bacterial clusters on amoebae migrating in biofilms generated by JR32, ΔlqsA , or ΔicmT , these clusters were barely present and much smaller on amoebae in biofilms formed by ΔlvbR and entirely absent in biofilms formed by ΔlqsR or ΔflaA (Fig. 6). The bacterial clusters on amoebae in ΔflaA biofilms were partially restored by the expression of plasmid-borne *flaA* in the mutant strain (Fig. S4D and E). Finally, the mCherry-producing parental strain JR32 clustered to *A. castellanii* also in presence of and upon competition with GFP-

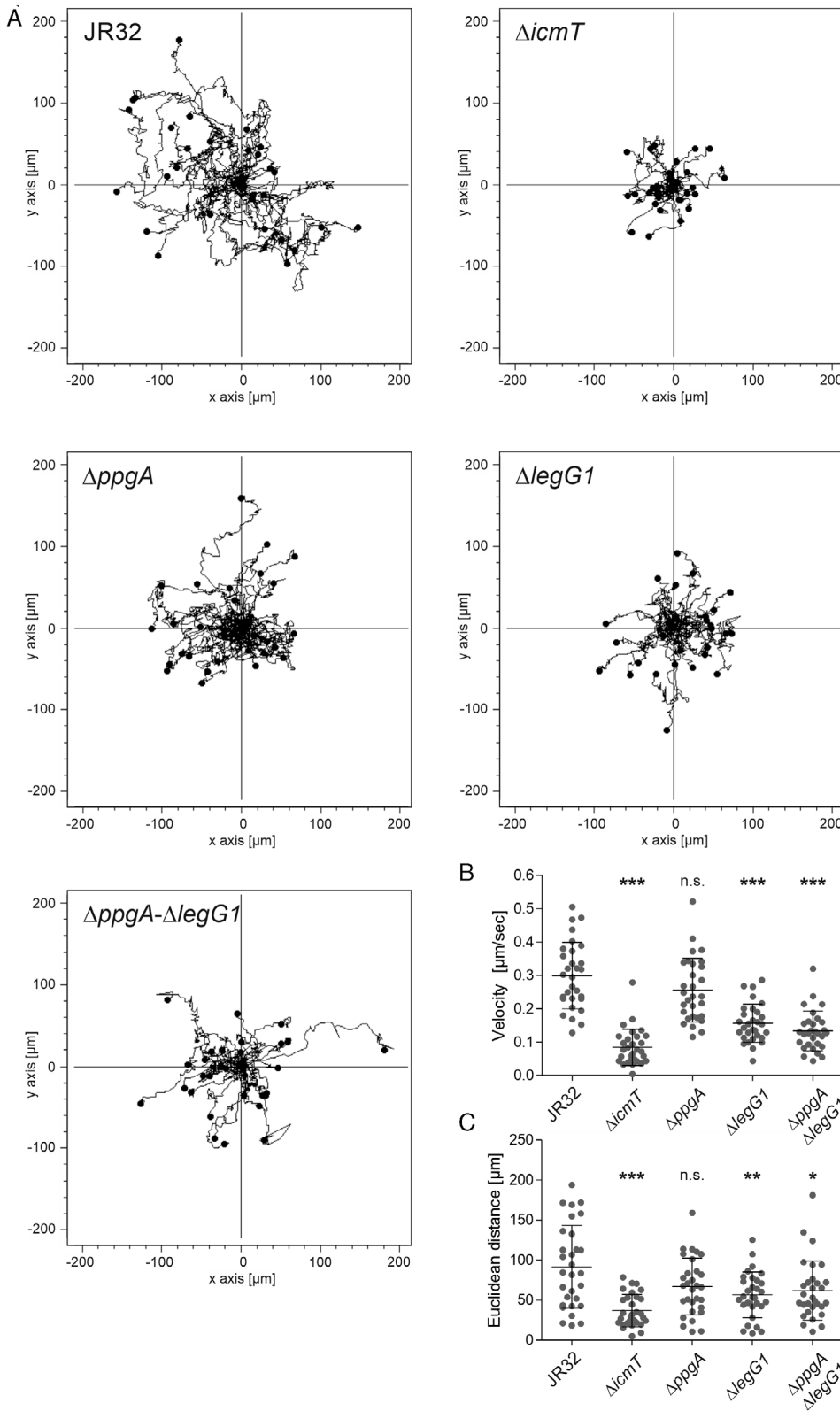


Fig. 5. The Icm/Dot T4SS and the effector LegG1 promote *A. castellanii* migration through *L. pneumophila* biofilms. Biofilms of *L. pneumophila* JR32, $\Delta icmT$, $\Delta ppgA$, $\Delta legG1$ or $\Delta ppgA-\Delta legG1$ mutant strains harbouring pNT28 (constitutive production of GFP) were grown in AYE medium at 25°C, *A. castellanii* was added to pre-formed biofilms after 6 days and amoeba migration was followed by confocal microscopy. A. Single amoeba migrating through biofilms were tracked and individually shown as a line in migration plots. B. The velocities and (C) Euclidean distances of migrating amoebae tracked in (A) were quantified. The data (B, C) are means and standard deviations of the mean derived from all tracked amoebae (n.s., not significant; * $p \leq 0.05$; ** $p \leq 0.01$; *** $p \leq 0.001$; one-way ANOVA with Tukey post-test; JR32 vs. mutant strains). Single amoebae were tracked in three biologically independent experiments with a total of $n = 30$ amoebae for each bacterial strain.

producing mutant strains (Fig. S6), indicating that the cluster phenotype is dominant. In summary, these results indicate that the regulatory proteins LvbR and LqsR as

well as flagellin (FlaA) not only promote the migration of amoebae in *L. pneumophila* biofilms but are also implicated in the formation of bacterial clusters on the

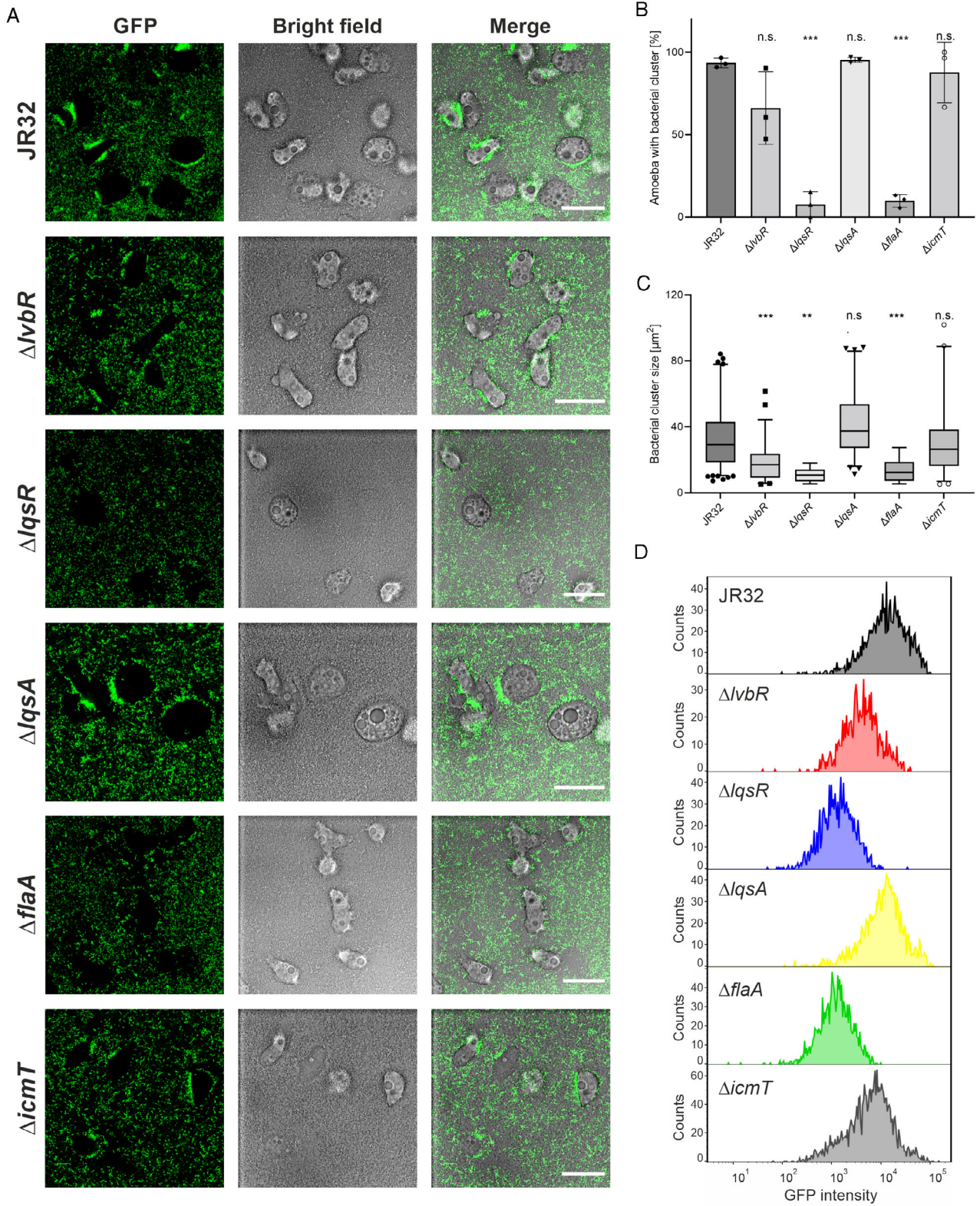


Fig. 6. Legend on next page.

migrating amoebae, while the autoinducer synthase LqsA and the lcm/Dot T4SS are dispensable for the phenotype.

Amoeba-adherent L. pneumophila clusters express motility and virulence genes

To further characterize the features of the *L. pneumophila* clusters on *A. castellanii* migrating in biofilms, we analysed the activity of promoters serving as prototypic proxies for motility (P_{flaA}), virulence (P_{sidC} , P_{ralF}), stress response (P_{6SRNA}) and replication (P_{csrA}). To this end, we constructed single GFP reporters, which produced the fluorescent protein under control of these promoters in AYE broth (Fig. S7A–E). The parental strain JR32 was transformed with transcriptional *gfp* fusions of the above promoters, and biofilms were grown in AYE medium for 6 days at 25°C. After addition of *A. castellanii* for ca. 3 h, the promoter activity was analysed by fluorescence microscopy (Fig. 7A). This approach revealed that the P_{flaA} , P_{sidC} and P_{ralF} promoters showed strong activity in the amoeba-adherent *L. pneumophila* clusters, while P_{6SRNA} and P_{csrA} were less or not active. Quantitative assessment of promoter activity by flow cytometry confirmed that P_{flaA} , P_{sidC} and P_{ralF} were strongly induced in amoeba-associated *L. pneumophila*, while P_{6SRNA} and P_{csrA} were less or not active (Fig. 7B and C, Fig. S5C).

We also tested dual GFP reporter constructs of P_{flaA} , P_{sidC} , P_{ralF} , P_{6SRNA} and P_{csrA} , which in parallel also constitutively produce mCherry. Of these constructs, only P_{flaA} and P_{6SRNA} produced a robust GFP signal, which was observed in *L. pneumophila* in broth (Fig. S8A and B, data not shown). Similar to the single reporter constructs, the P_{flaA} promoter was induced in the amoeba-adherent *L. pneumophila* clusters in biofilms, while P_{6SRNA} was not (Fig. S8C). Moreover, usage of the P_{flaA} dual reporter construct confirmed that amoeba-adherent *L. pneumophila* clusters were most robustly formed in biofilms formed by strain JR32, less in $\Delta lvbR$ biofilms and barely in biofilms formed by the $\Delta lqsR$ mutant strain (Fig. S8D). Taken together, these findings are in agreement with the notion that the bacteria in the clusters are in stationary growth phase and motile. In summary, the

individual bacteria in the *L. pneumophila* clusters on *A. castellanii* migrating in biofilms express the P_{flaA} , P_{sidC} and P_{ralF} promoters, and therefore, are likely in the non-growing, transmissive and virulent phase.

Discussion

In this study, we investigated the role of the *L. pneumophila* genotype on biofilm formation and morphology, the migration of amoebae within biofilms and the occurrence of amoeba-associated bacterial clusters (Table 1). We found that the transcription factor LvbR, the quorum-sensing response regulator LqsR, the bacterial flagellum (FlaA) and the lcm/Dot T4SS regulate the speed and (except for FlaA) the migration distance of *A. castellanii* moving through *L. pneumophila* biofilms (Figs 4 and 5). Furthermore, LvbR, LqsR and FlaA also regulate the adherence and cluster formation of *L. pneumophila* on the amoeba surface, and the clusters comprise P_{flaA}^- and P_{sidC}^- -positive, i.e. motile and virulent bacteria (Figs 6 and 7).

Intriguingly, the migration of amoebae through *L. pneumophila* biofilms was positively correlated to the virulence of the bacterial strains (Table 1). *Acanthamoeba castellanii* moved slower and less vigorously through biofilms formed by the $\Delta lvbR$ and $\Delta lqsR$ regulatory mutants (Fig. 4), which are impaired for virulence (Tiaden *et al.*, 2007; Hochstrasser *et al.*, 2019), and also through biofilms formed by the avirulent $\Delta icmT$ T4SS mutant strain, or biofilms formed by strains lacking the lcm/Dot-translocated effectors LegG1 or LegG1 and PpgA (Fig. 5). LegG1 and PpgA are RCC1 repeat effectors, which localize to LCVs or the plasma membrane, target the activation cycle of the small GTPase Ran and activate Ran either at the LCV or the plasma membrane respectively (Rothmeier *et al.*, 2013; Swart *et al.*, 2020b). The activation of Ran GTPase by the *L. pneumophila* RCC1 repeat effectors promotes microtubule stabilization, LCV motility and cell migration (Rothmeier *et al.*, 2013; Simon *et al.*, 2014; Swart *et al.*, 2020a). Given the cell migration phenotypes of the $\Delta legG1$, $\Delta ppgA$ and $\Delta legG1-\Delta ppgA$ mutant strains, presumably the effectors also positively regulate the microtubule

Fig. 6. LvbR, LqsR and FlaA determine *L. pneumophila* cluster formation on *A. castellanii*. Biofilms of *L. pneumophila* JR32, $\Delta lvbR$, $\Delta lqsR$, $\Delta lqsA$, $\Delta flaA$ or $\Delta icmT$ mutant strains harbouring pNT28 (constitutive production of GFP) were grown for 6 days in AYE medium at 25°C, and *A. castellanii* was added to preformed biofilms.

A. Bacterial adherence and cluster formation were monitored in biofilms containing amoebae by confocal microscopy above the dish bottom. The images shown are representative of three independent experiments. Scale bars, 30 μ m.

B. Percentage of amoebae with bacterial cluster (or cluster-positive amoebae) in the total amoeba population. The columns display the mean value of three biological replicates (in dots) with standard deviations.

C. Quantification by fluorescence microscopy of cluster size on cluster-positive amoebae. The box-and-whisker plots display 5th to 95th percentiles (whiskers), median and quartiles (box) of the pooled results from three biologically independent experiments with a total analysed number of amoebae $n = 124$ (JR32), $n = 60$ ($\Delta lvbR$), $n = 9$ ($\Delta lqsR$), $n = 66$ ($\Delta lqsA$), $n = 8$ ($\Delta flaA$), or $n = 48$ ($\Delta icmT$). For (B) and (C): n.s., not significant; * $p \leq 0.05$; ** $p \leq 0.01$; *** $p \leq 0.001$; one-way ANOVA with Tukey post-test; JR32 vs. mutant strains.

D. Quantification by flow cytometry (counts vs. fluorescence intensity) of amoeba-associated, GFP-positive *L. pneumophila* (JR32, $\Delta lvbR$, $\Delta lqsR$, $\Delta lqsA$, $\Delta flaA$ or $\Delta icmT$ harbouring pNT28) using FlowJo software (protocol #1, see Materials and Methods).

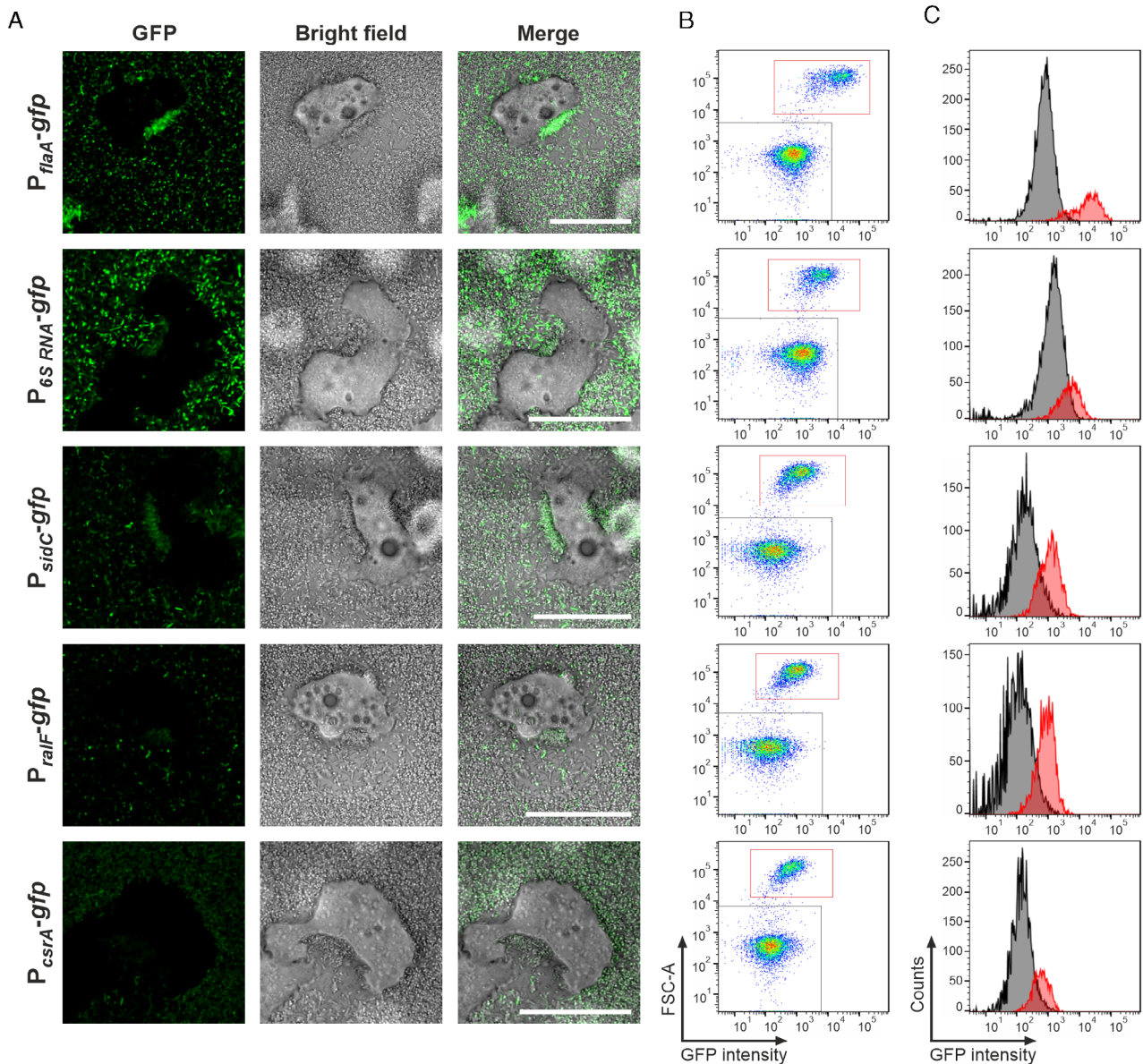


Fig. 7. Amoeba-adherent *L. pneumophila* clusters express motility and virulence genes.

A. Biofilms of *L. pneumophila* JR32 harbouring promoter-reporter plasmids P_{flaA} -*gfp* (pCM009), $P_{6S RNA}$ -*gfp* (pRH049), P_{sidC} -*gfp* (pRH035), P_{ralF} -*gfp* (pRH032) or P_{csrA} -*gfp* (pRH031) were grown in AYE medium for 6 days. *Acanthamoeba castellanii* was added to preformed biofilms and confocal microscopy images of amoebae with adherent bacterial clusters were acquired close to the bottom of microscopy dishes. The images shown are representative of at least two independent experiments. Scale bars, 30 μ m. Quantification by flow cytometry of GFP-positive *L. pneumophila* JR32 harbouring promoter reporters (P_{flaA} , $P_{6S RNA}$, P_{sidC} , P_{ralF} , or P_{csrA}) using FlowJo software: (B) forward scatter area (FCS-A) versus fluorescence intensity, or (C) counts versus fluorescence intensity [amoebae-associated (red) and non-associated (black)] (protocol #2, see Materials and Methods).

Table 1. Summary of biofilm-amoeba interaction and virulence phenotypes.

Phenotypes	JR32	$\Delta lvrR$	$\Delta lqsR$	$\Delta lqsA$	$\Delta flaA$	$\Delta icmT$
Biofilm architecture ^a	p	m	p	p	p	p
Amoeba migration	++	+	+	++	+	+
Cluster formation	++	+	-	++	-	++
Bacterial virulence	++	+	+	++	+	-

^aAbbreviations: p, 'patchy'; m, 'mat'-like.

cytoskeleton and cell migration of *A. castellanii* moving through biofilms.

The amoeba speed was also impaired in biofilms formed by *L. pneumophila* lacking *flaA* encoding bacterial flagellin (FlaA), and thus, was positively correlated to the presence of FlaA (Fig. 4). Moreover, the amoebae moved with a lower speed through biofilms formed by the Δ *lqsR* strain compared to Δ *lvbR* (Fig. 4B), in agreement with the decreasingly pronounced role of LqsR and LvbR in regulating P_{flaA} (Fig. 2B and C). However, the amoebae moved with an even lower speed through Δ *lqsR* biofilms compared to Δ *flaA*. Thus, FlaA is not essential for amoeba migration through *L. pneumophila* biofilms and LqsR likely regulates other factors implicated in the process.

The mechanism, by which FlaA and the flagellum promote amoeba migration through biofilms is unclear. Perhaps, the amoebae detect and respond to the 'pathogen-associated molecular pattern' flagellin. Overall, the enhanced migration of *A. castellanii* in biofilms formed by virulent *L. pneumophila* might be a 'flight' reaction. Such a reaction would expand the behavioural repertoire of biofilm-interacting amoebae, beyond 'grazing' on these bacterial communities (Ronn *et al.*, 2002; Huws *et al.*, 2005; Matz and Kjelleberg, 2005).

An obvious explanation for the biofilm genotype-dependent differences in the migration of amoebae might be distinct biofilm architectures and structures. The homogenous 'mat'-like biofilm architecture of Δ *lvbR* biofilms (Hochstrasser *et al.*, 2019) could cause slower amoeba migration, while amoebae migrate faster through 'patchy' biofilms with interspersed clusters formed by wild-type JR32 bacteria and some mutant strains. However, this seems not to be the case, since the patchy biofilms formed by the Δ *lqsR*, Δ *flaA* and Δ *icmT* mutant strains (Fig. 3) also sustained only slow amoeba migration. Thus, the biofilm morphology and structure do not seem to correlate with the features of amoeba migration. However, we did not label any matrix components, e.g. exopolysaccharides, protein or eDNA, which might account for the differential migration of the amoebae. Hence, the mechanism(s), by which the lack of the regulatory factors (LvbR, LqsR) impede amoeba migration is unclear.

As a general mechanistic concept, LvbR- or LqsR-regulated bacterial factor(s) or feature(s) might trigger and affect the amoeba migration dynamics in *L. pneumophila* biofilms. *Legionella pneumophila* strains lacking *lvbR* (Hochstrasser *et al.*, 2019) or *lqsR* (Tiaden *et al.*, 2007) are impaired for virulence, and both regulatory factors control the production of Icm/Dot-translocated effector proteins. In sessile *L. pneumophila*, some Icm/Dot-translocated effectors are less abundantly produced by the Δ *lvbR* or Δ *lqsR* mutant strains compared

to the parental strain (Fig. S1). These include the astacin protease LegP (de Felipe *et al.*, 2008), the deAMPylase SidD (Neunuebel *et al.*, 2011; Tan and Luo, 2011), the ubiquitin ligase SdeA (Qiu *et al.*, 2016), the Rab1 GEF RalF (Nagai *et al.*, 2002) and the protein kinase Lpg2603 (Sreelatha *et al.*, 2020). SdeA and RalF are *L. pneumophila* effector proteins typically produced in the post exponential growth phase, while LegP and SidD are non-differentially produced (Aurass *et al.*, 2016). The lack (or lower abundance) of specific effectors might account for the lower migration speed of *A. castellanii* through biofilms formed by the Δ *lvbR* or Δ *lqsR* mutants, analogously to what has been observed for the Δ *icmT*, Δ *legG1*, Δ *ppgA* and Δ *legG1*- Δ *ppgA* mutant strains (Fig. 5). Alternatively or additionally, the Δ *lvbR* or Δ *lqsR* mutants might be defective for the production of adhesins or components of the extracellular biofilm matrix. As the amoebae were added to *L. pneumophila* biofilms formed over 6 days, such bacterial structures might indeed play a role in determining amoeba migration.

In previous studies, the inhibition of migration and chemotaxis of *D. discoideum*, macrophages and neutrophils was positively correlated with the virulence of *L. pneumophila* (Simon *et al.*, 2014; Hochstrasser *et al.*, 2019). While the parental strain JR32 dose-dependently inhibited phagocyte migration in under-agar and transwell assays, the Δ *icmT* mutant did not. Compared to JR32, the less virulent Δ *lvbR* mutant strain inhibited *D. discoideum* migration less efficiently, but more efficiently than Δ *icmT* (Hochstrasser *et al.*, 2019). *Legionella pneumophila* Δ *legG1* even hyper-inhibited phagocyte migration, indicating that microtubule stabilization by the RCC1 repeat effector promotes cell motility (Simon *et al.*, 2014). As outlined above, presumably the RCC1 repeat effectors also positively regulate the microtubule cytoskeleton and cell migration of *A. castellanii* moving through biofilms (Fig. 5).

In the previous migration and chemotaxis studies, the phagocytes were infected with *L. pneumophila* strains for 1 h prior a 4 h migration/chemotaxis assay, and therefore, had already taken up bacteria (Simon *et al.*, 2014; Hochstrasser *et al.*, 2019). Accordingly, the effect of *L. pneumophila* on eukaryotic cell migration seems to depend on whether planktonic bacteria are being taken up or cluster extracellularly. In agreement with this notion, the efficient uptake of *L. pneumophila* by amoebae and macrophages is promoted by LvbR (Hochstrasser *et al.*, 2019), LqsR (Tiaden *et al.*, 2007; Tiaden *et al.*, 2008), the flagellum (FlaA) (Dietrich *et al.*, 2001) and the Icm/Dot T4SS (Hilbi *et al.*, 2001; Weber *et al.*, 2006).

Another intriguing observation was the adherence and cluster formation of *L. pneumophila* on amoebae migrating in biofilms. Cluster formation was controlled by LvbR,

LqsR and FlaA, but not by LqsA or the lcm/Dot T4SS, since the $\Delta lvbR$, $\Delta lqsR$ and $\Delta flaA$ mutants were defective for cluster formation, while $\Delta lqsA$ or $\Delta icmT$ formed clusters like the parental strain JR32 (Fig. 6). *Legionella pneumophila* lacking *flaA* was severely impaired for cluster formation, and thus, FlaA might act as an adhesin and promote binding to the amoebae. While the bacterial flagellum is known to act as an adhesion factor (Haiko and Westerlund-Wikstrom, 2013), it is unclear whether the flagellum *per se* or flagella-based motility is required for cluster formation of *L. pneumophila*. LvbR and LqsR regulate the production of the *L. pneumophila* flagellum filament protein FlaA (Lpg1340) and the transcription of *flaA* (Fig. S1, Fig. 2B and C), and thus, possibly contribute to cluster formation on amoebae. Finally, in agreement with a role of LqsR for the regulation of bacterial adherence and cluster formation, LqsR (but not LqsA) was previously found to be a regulator of 'extracellular filaments', which form a network and prevent the sedimentation of the bacteria (Tiaden *et al.*, 2007).

In addition to the flagellum, other *L. pneumophila* factors possibly promote bacterial cluster formation on the amoeba surface in the biofilms. LvbR as well as LqsR are positive regulators of Tfp pili (pilus retraction ATPase PilT, Lpg0987) (Fig. S1), which might function as adhesins. Lcl (Lpg2644) is another candidate, since this adhesin mediates the adherence to host cells (Vandersmissen *et al.*, 2010) and is implicated in bacterial adhesion during biofilm formation (Duncan *et al.*, 2011; Mallegol *et al.*, 2012). Intriguingly, Lcl is less abundant in biofilms formed by the $\Delta lvbR$ mutant strain (Fig. S1), which might contribute to the reduced adherence and cluster formation of the mutant on amoebae (Fig. 6). In general, bacterial factors contribute individually or in concert to the extracellular biofilm matrix, which might promote adherence and clustering of *L. pneumophila* on the surface of amoebae.

The function of the *L. pneumophila* clusters on amoebae in biofilms is unclear. Successful and efficient intracellular replication of *L. pneumophila* depends on adherence to host cells (Cirillo *et al.*, 2001; Chang *et al.*, 2005; Duncan *et al.*, 2011), and thus, cluster formation might facilitate *L. pneumophila* uptake by host cells within biofilms. Alternatively or additionally, bacterial adherence to amoebae and subsequent cell migration possibly helps *L. pneumophila* to disseminate in the environment. A similar clustering phenomenon was recently reported for planktonic *Listeria monocytogenes*, a foodborne, extracellular Gram-positive bacterium. *Listeria monocytogenes* formed densely packed aggregates on *A. castellanii* and *A. polyphaga* called 'backpacks', and the formation was dependent on flagella-based motility (Doyscher *et al.*, 2013). However, *L. monocytogenes* does not persist in *Acanthamoeba* spp. and simply

serves as food for the amoebae. In contrast, *L. pneumophila* does not serve as food but rather consumes and destroys the amoebae. Hence, *L. pneumophila* might subvert a mechanism employed by *A. castellanii* to trap and feed on bacteria, in order to efficiently infect protozoan host cells.

Comparative proteomics of biofilms formed by JR32, $\Delta lvbR$ or $\Delta lqsR$ mutant strains revealed that LvbR and LqsR are implicated in the regulation of the flagellum, the Lvh T4SS, lcm/Dot-translocated effectors and proteins encoded by the 133 kb genomic island regions I and II (Fig. S1). Comparative transcriptomics of sessile and planktonic JR32, $\Delta lvbR$ or $\Delta lqsR$ mutant strains indicated similar target genes of the regulators, including the 133 kb genomic island region I (*lpg0973-1005*) and region II (*lpg1006-1096*), the *lvh* region (*lpg1244-1259*) and various genes involved in flagellar biosynthesis (*lpg1216-1226*, *lpg1337-1340*, *lpg1759-1763*, *lpg1780-1789* and *lpg1791-1792*) (Hochstrasser *et al.*, 2019). Taken together, these studies provide insights on the components of *L. pneumophila* biofilms and their interactions with amoebae. Further studies will address the functions and mechanisms underlying the migration of amoebae in *L. pneumophila* biofilms and bacterial cluster formation on the amoebae.

Experimental procedures

Growth and motility of bacteria, cultivation of amoebae

Legionella pneumophila strains (Table 2) were grown on CYE agar plates for 3 days (Feeley *et al.*, 1979), or were grown to exponential phase in liquid cultures with *N*-(2-acetamido)-2-aminoethanesulfonic acid-buffered yeast extract (AYE) medium (Horwitz, 1983) at 37°C on a wheel (80 rpm) for approximately 18 h. AYE medium was supplemented with chloramphenicol (Cm; 5 µg ml⁻¹) to maintain plasmids if required.

Bacterial motility was assessed basically as described (Schell *et al.*, 2016). Briefly, *L. pneumophila* JR32 or the $\Delta lvbR$ or $\Delta lqsR$ mutant strains were grown for 3 days on CYE/Cm agar plates. Liquid cultures were inoculated in AYE medium at an OD₆₀₀ of 0.1 and grown for 21 h at 37°C. After 21 h, bacterial cultures were diluted to an OD₆₀₀ of 0.15, and 700 µl were filled into ibidi-microscopy dishes. Bacteria were tracked for 90 with 1.298 s intervals using a Leica SP8 confocal microscope (63× oil objective). Bacterial motility was visualized using the ImageJ software. The Movies S1–S3 are representative of two independent experiments.

Acanthamoeba castellanii (ATCC 30234, lab collection) was cultured in PYG medium (Moffat and Tompkins, 1992; Segal and Shuman, 1999) at 23°C

using protease from Becton Dickinson Biosciences and yeast extract from Difco.

Molecular cloning

Plasmids used in this study are listed in Table 2. DNA cloning was carried out according to standard protocols, plasmids were isolated using commercially available kits (Qiagen, Macherey-Nagel), and DNA fragments were amplified using the primers listed in Table S1. All the constructs were verified by DNA sequencing. The complementation plasmids pRH022 (P_{IvbR} - $IvbR$) and pSB001 (P_{flaA} - $flaA$) were generated by amplifying the corresponding gene with its putative natural promoter region using the primer pair oRH040/oRH041 or oRH174/oRH175 and pAK18 or genomic JR32 DNA as template. The NEBuilder HiFi DNA Assembly reaction was used to clone the PCR product into BspQI-digested pCM009 (Schell *et al.*, 2016) resulting in pRH022 or into

BamHI-digested pNT31 (Tiaden *et al.*, 2010b) thereby replacing P_{IqsS} - $IqsS$ and resulting in pSB001.

Single reporter constructs pRH031, and pRH049 containing a transcriptional fusion P_{CSRA} - gfp (ASV), or P_{6SRNA} - gfp (ASV) were generated by PCR amplification of the putative promoter regions from genomic JR32 DNA using the primer pair oRH128/oRH129, or oRH215/oRH216. The putative promoter regions were defined as the upstream region of the corresponding genes with the following sizes: P_{CSRA} (515 bp, $Ipg0781$) and P_{6SRNA} (534 bp, $ssrS$, between $Ipg0877$ and $Ipg0876$). The PCR products were cloned into SacI- and XbaI-digested pCM009 (Schell *et al.*, 2016) using the NEBuilder HiFi DNA Assembly reaction, thereby replacing P_{flaA} .

For construction of the dual reporter constructs pRH046, pRH047 and pRH050 harbouring P_{CSRA} - gfp (AAV), P_{ralF} - gfp (AAV) or P_{sidC} - gfp (AAV), the putative promoter regions were amplified by PCR with the primer pairs oRH182/oRH210, oRH180/oRH211 or oRH217/

Table 2. Bacterial strains and plasmids used in this study.

Strain or plasmid	Relevant properties ^a	Reference
<i>E. coli</i>		
TOP10		Invitrogen
<i>L. pneumophila</i>		
AK01 ($\Delta IqsT$)	JR32 $IqsT::Km$	Kessler <i>et al.</i> (2013)
AK02 ($\Delta IqsS$ - $\Delta IqsT$)	JR32 $IqsS::Km IqsT::Gm$	Kessler <i>et al.</i> (2013)
AK03 ($\Delta IvbR$)	JR32 $IvbR::Km$	Hochstrasser <i>et al.</i> (2019)
ER01 ($\Delta legG1$)	JR32 $legG1::Km$	Rothmeier <i>et al.</i> (2013)
GS3011 ($\Delta icmT$)	JR32 $icmT3011::Km$	Segal and Shuman (1998)
JR32	<i>L. pneumophila</i> Philadelphia-1, serogroup 1, salt-sensitive isolate of AM511	Sadosky <i>et al.</i> (1993)
LS01 ($\Delta ppgA$ - $\Delta legG1$)	JR32 $ppgA::Gm legG1::Km$	Swart <i>et al.</i> (2020b)
LS03 ($\Delta ppgA$)	JR32 $ppgA::Km$	Swart <i>et al.</i> (2020b)
NT02 ($\Delta IqsA$)	JR32 $IqsA::Km$	Tiaden <i>et al.</i> (2010b)
NT03 ($\Delta IqsR$)	JR32 $IqsR::Km$	Tiaden <i>et al.</i> (2007)
NT05 ($\Delta IqsS$)	JR32 $IqsS::Km$	Tiaden <i>et al.</i> (2010b)
$\Delta flaA$	JR32 $flaA::Km$	Weber <i>et al.</i> (2012)
Plasmids		
pAK18	pMMB207C- P_{IvbR} - $IvbR$, gfp (constitutive)	Hochstrasser <i>et al.</i> (2019)
pCM009	pMMB207C- P_{flaA} - gfp (ASV)	Schell <i>et al.</i> (2016)
pNP102	pMMB207C, $\Delta lacI^q$, $mcherry$ (constitutive)	Steiner <i>et al.</i> (2017)
pNT28	pMMB207C, gfp (constitutive)	Tiaden <i>et al.</i> (2007)
pNT31	pMMB207C- P_{IqsS} - $IqsS$, gfp (constitutive)	Tiaden <i>et al.</i> (2010b)
pRH022	pMMB207C- P_{IvbR} - $IvbR$ - P_{flaA} - gfp (ASV)	This study
pRH031	pMMB207C- P_{CSRA} - gfp (ASV), Cm	This study
pRH032	pMMB207C- P_{ralF} - gfp (ASV), Cm	Striednig <i>et al.</i> (2021)
pRH035	pMMB207C- P_{sidC} - gfp (ASV), Cm	Striednig <i>et al.</i> (2021)
pRH046	pMMB207C- P_{CSRA} - gfp (AAV), $mcherry$ (constitutive), Cm	This study
pRH047	pMMB207C- P_{ralF} - gfp (AAV), $mcherry$ (constitutive), Cm	This study
pRH049	pMMB207C- P_{6SRNA} - gfp (ASV), Cm	This study
pRH050	pMMB207C- P_{sidC} - gfp (AAV), $mcherry$ (constitutive), Cm	This study
pSB001	pMMB207C- P_{flaA} - $flaA$, gfp (constitutive)	This study
pSN7	pMMB207C- P_{flaA} - gfp (AAV), $mcherry$ (constitutive), Cm	Personnic <i>et al.</i> (2019)
pSN25	pMMB207C- P_{6SRNA} - gfp (AAV), $mcherry$ (constitutive), Cm	Personnic <i>et al.</i> (2021)

^aAbbreviations: Cm, chloramphenicol resistance; Km, kanamycin resistance; Gm, gentamicin resistance.

oRH218 and pRH031, pRH032 or pRH035 as template. The putative promoter regions were defined as the upstream region of the corresponding genes with the following sizes: P_{ralF} (515 bp, *lpg1950*) and P_{sidC} (507 bp, *lpg2511*). The resulting PCR products were inserted into BamHI- and BglII-digested pSN7 (Personnic et al., 2019) using the NEBuilder HiFi DNA Assembly reaction, thereby exchanging P_{flaA} .

Kinetics of GFP reporter constructs

Legionella pneumophila strains (Table 2) harbouring GFP reporter constructs (single reporters: pCM009, pRH022, pRH031, pRH032, pRH035, pRH049, or dual reporters: pRH046, pRH047, pSN7, pSN25) were grown on CYE/Cm agar plates for 3 days, followed by cultivation in AYE/Cm medium at 37°C on a rotating wheel (80 rpm) for approximately 18 h. The strains were diluted in AYE/Cm medium to an initial OD₆₀₀ of 0.2, and 100 µl was distributed in triplicates into wells of a black clear bottom 96-well plate (polystyrene, 353219, Falcon). The plate was incubated at 25°C or 37°C while orbitally shaking, and GFP fluorescence (excitation, 485 nm; emission, 528 nm; gain, 50 or 100) as well as OD₆₀₀ (bacterial growth) were measured over time using a microplate reader (Synergy H1 or Cytation5 Hybrid Multi-Mode Reader, BioTek). A blank value (AYE medium) was subtracted from all values, and numbers are expressed as relative fluorescence units (RFU), OD₆₀₀ or RFU/OD₆₀₀ quotient.

Legionella pneumophila biofilm formation

For analysis of biofilm architecture or *Legionella*–amoeba interactions, *L. pneumophila* biofilms were prepared, monitored and analysed as described (Hochstrasser and Hilbi, 2019). Briefly, *L. pneumophila* strains harbouring pNT28, pNP102 or single/dual reporter constructs (Table 2) were grown for 3 days at 37°C on CYE agar plates supplemented with Cm (5 µg ml⁻¹) and subsequently cultivated in AYE/Cm medium on a rotating wheel (80 rpm) at 37°C for approximately 17–18 h. The exponential phase bacteria were inoculated at an optical density (OD₆₀₀) of 0.3 in 2 ml AYE/Cm medium placed into ibiTreat microscopy dishes (ibidi), incubated at 25°C for the time indicated while avoiding any mechanical disturbance, and optionally stained with DAPI (1 µg ml⁻¹). The biofilm architecture was monitored by confocal fluorescence microscopy (Leica TCS SP5, 63× oil objective) by acquiring images at the dish bottom (0 µm, attachment layer) or at a level of 4 µm above the dish bottom. For competition assays, biofilms were generated analogously with an inoculation OD₆₀₀ of 0.15 for each strain (start ratio of 1:1) using *L. pneumophila* JR32 harbouring

pNP102 (mCherry) and mutant strains harbouring pNT28 (GFP).

To quantify biofilm formation, *L. pneumophila* strains harbouring pNT28 were left to form biofilms at 25°C for 6 days as described above. The biofilms were re-suspended by excessive pipetting until the bottom of the dish appeared clear. The suspension was transferred into a falcon tube, excessively vortexed (to avoid that the bacteria stick together), and the OD₆₀₀ was determined (usually 3.3–4.1). Subsequently, the suspension was diluted 1:100 (beads: bacteria) with a microsphere standards suspension (Bacteria counting kit, Invitrogen). The biofilm mass (bacteria ml⁻¹) was quantified using a Fortessa II flow cytometer and Diva software. Bacteria and microsphere standard were determined by employing a forward (FSC, 650 V) and sideward scatter (SSC, 230 V), with a threshold of 200 each. Additionally, GFP production (Blue 530_30, 350 V) was examined to identify *L. pneumophila*. 100000 events of each resuspended biofilm were recorded. Immediately before measuring, samples were strongly vortexed for 8 s. The data were analysed with the software FlowJo. The gating protocol was as follows: The beads were identified using a control sample (AYE/Cm without bacteria) that was supplemented with beads as a reference (gate 1, FSC vs. SSC). The number of events counted in the microsphere gate provides an accurate estimate of the volume analysed. The *L. pneumophila* populations were determined in pseudocolour graphs (gate 2, GFP vs. FSC) using a resuspended biofilm sample (of parental strain JR32) without beads as a reference. Bacterial density in the biofilm was determined from the ratio of *L. pneumophila* (gate 2) to beads (gate 1).

Legionella–amoeba interactions

For confocal fluorescence microscopy, *A. castellanii* amoebae were detached after 2–3 days of growth and diluted in fresh PYG medium to a density of 1.5×10^5 cells ml⁻¹. 1 ml of amoebae suspension was carefully added to preformed *L. pneumophila* biofilms grown for 6 days (as described above) resulting in a final amoebae concentration of 5×10^4 cells ml⁻¹ in the dish. The dish was incubated for approximately 3 h (images) or 15 min (time-lapse stacks) at 25°C to allow the amoebae to settle toward the bottom of the dish. *Legionella*–amoeba interactions were visualized by confocal fluorescence microscopy (Leica TCS SP5, 63× oil objective) by acquiring images or time-lapse stacks and 3D images or movies were generated using the program ImageJ. For further analysis of amoeba migration, single-cell tracking was manually performed in the bright field channel using time-lapse stacks and the program ImageJ. Time series of ca. 10 amoebae localizing above the dish bottom were

recorded for the same time (25 or 30 min). Only viable, irregularly shaped amoebae were considered (rounded and clustered amoebae were ignored, except in the case of the *ΔicmT* mutant strain, which caused a larger portion of the amoebae to round up). The ibidi program 'Chemotaxis and Migration Tool' was used to generate migration plots and to quantify the amoeba velocity (Hochstrasser and Hilbi, 2019).

The total number of amoebae and the number of amoebae with a bacterial cluster (or cluster-positive amoebae) were counted manually from the microscopy images of *L. pneumophila* strains harbouring pNT28 (constitutive production of GFP). The percentage of cluster-positive amoebae was assessed for each of three independent biological experiments. Subsequently, for each cluster-positive amoeba, the cluster size was quantified with ImageJ (Version 1.53f51). In brief, a detection mask was created for each microscopy image with its GFP channel ('Image' > 'Adjust' > 'Threshold: 100–255'). Then the size of all clusters in the image was analysed using 'Analyse particle' function ('Analyse' > 'Analyse particle' > 'Size 10 micron – Infinity'). The size of clusters was quantified for *L. pneumophila* strains harbouring pNT28 (constitutive production of GFP) in three independent biological experiments.

For flow cytometry, *A. castellanii* amoebae were added to preformed biofilms grown for 6 days at 25°C as described above, optionally stained with DAPI (1 μg ml⁻¹) and incubated for approximately 2–3 h at 25°C. Biofilms were harvested by resuspending the bacteria and amoebae, followed by centrifugation for 10 min at 100 g (biofilms including amoebae), or for 5 min at 4400 rpm (control biofilms without amoebae). Samples were fixed with 300 μl 4% PFA in PBS for approximately 30 min at RT, washed once in 300 μl PBS and resuspended in 150 μl PBS for flow cytometry analysis.

The size of GFP-positive *L. pneumophila* clusters on *A. castellanii* in bacterial biofilms was quantified by flow cytometry as amoeba-associated fluorescence using a Fortessa II flow cytometer (BD LSR II Fortessa) and Diva software. Different populations were identified employing a forward (FSC, 430 V) and sideward scatter (SSC, 270 V) gating, with a threshold of 200 each, and 10000 events per sample were recorded. Furthermore, the populations were examined for GFP production [Blue 530_30, 350 V (gating protocol #1) or 400 V (gating protocol #2)]. The data were analysed with the software FlowJo. The gating protocol #1 for strains containing plasmid pNT28 was as follows: amoeba populations were identified using an amoeba only sample as a reference (gate 1). Cluster formation was visualized by a GFP-shift of the amoebae population visible in pseudocolour graphs (including the *L. pneumophila* population) and histograms (not including the *L. pneumophila*

population, gate 1). The gating protocol #2 for strains containing promoter expression constructs was as follows: amoebae/*L. pneumophila* populations were identified using amoebae/*L. pneumophila* only samples as a reference (gates 1 and 2). The GFP signal of the two populations was visualized together in a histogram (gate 1 and 2) and in pseudocolour graphs (no gating).

Comparative proteomics

Biofilms of *L. pneumophila* JR32, *ΔlvrR* and *ΔlqsR* were initiated as described above and incubated for 6 days at 25°C. The biofilms were harvested by resuspending the bacteria, followed by centrifugation (5 min, 12850 g, 4°C) and resulting supernatants (designated 's', extracellular) and cell pellets (designated 'p', intracellular) were analysed separately.

For extracellular sample preparation, proteins in 1 ml of supernatant were enriched using StrataClean beads and eluted by the use of a 1D-SDS gel according to the established protocol for GeLC-MS samples (Bonn *et al.*, 2014). Cell pellets (intracellular samples) were resuspended in TE-buffer pH 7.4 (50 mM Tris, 10 mM EDTA) and disrupted by bead beating. After centrifugation the protein concentration was determined using the Bradford assay and 20 μg protein was in solution digested (Maass *et al.*, 2011) and purified using C₁₈-Stage tips (Thermo Fisher Scientific). Extracellular proteins (with three biological replicates for every sample) and intracellular proteins (with three biological replicates and three technical replicates each for every sample) were analysed with a QExactive-Mass spectrometer. Peptide samples were injected with the same volume to allow label-free relative protein quantification between biological samples.

To process the data, *.raw files were searched against the database using MaxQuant (1.6.0.16). The database for *L. pneumophila* Philadelphia-1 was downloaded from Uniprot on March 17th, 2017 and supplemented with the *LvrR* sequence and common laboratory contaminations resulting in 2973 entries. The results were filtered using 1% FDR in MaxQuant and at least two unique peptides were necessary for protein identification (filtered in Perseus vs. 1.5.3.0). For quantification the protein had to be detected in at least two replicates of one sample. Log₂-transformed LFQ-values as proxy for protein abundance were exported and used for statistical analysis in TMEV. Only proteins with a minimal log₂-fold change of -0.8 or 0.8 compared to JR32 were considered. In cases, where proteins were detected in *ΔlvrR* or *ΔlqsR* but not in JR32 biofilms ('on'), or where proteins were detected in JR32 but not in *ΔlvrR* or *ΔlqsR* biofilms ('off'), the maximum values of 2^{7.4} and 2⁻⁵ were used as

ratios and coloured dark blue or dark red in the heat map (Fig. S1) respectively.

Acknowledgements

The work in the group of H.H. was supported by the Swiss National Science Foundation (SNF; 31003A_175557, 310030_200706), the Novartis Foundation for Medical-Biological Research (21C165). The work in the group of D.B. was supported by the Federal Ministry of Education and Research (BMBF; grant 031A410B). Open Access Funding provided by Universität Zurich.

Data Availability

The MS proteomics data discussed in this publication have been deposited to the ProteomeXchange Consortium via the PRIDE partner repository (Vizcaino *et al.*, 2016; Perez-Riverol *et al.*, 2019) with the dataset identifier PXD030337 (Reviewer account details: Username, reviewer_pxd030337@ebi.ac.uk; Password, a2Q4ygNx).

References

- Abdel-Nour, M., Duncan, C., Low, D.E., and Guyard, C. (2013) Biofilms: the stronghold of *Legionella pneumophila*. *Int J Mol Sci* **14**: 21660–21675.
- Abu Khweek, A., and Amer, A.O. (2018) Factors mediating environmental biofilm formation by *Legionella pneumophila*. *Front Cell Infect Microbiol* **8**: 38.
- Albert-Weissenberger, C., Sahr, T., Sismeiro, O., Hacker, J., Heuner, K., and Buchrieser, C. (2010) Control of flagellar gene regulation in *Legionella pneumophila* and its relation to growth phase. *J Bacteriol* **192**: 446–455.
- Aurass, P., Gerlach, T., Becher, D., Voigt, B., Karste, S., Bernhardt, J., *et al.* (2016) Life stage-specific proteomes of *Legionella pneumophila* reveal a highly differential abundance of virulence-associated Dot/Icm effectors. *Mol Cell Proteomics* **15**: 177–200.
- Bigot, R., Bertaux, J., Frere, J., and Berjeaud, J.M. (2013) Intra-amoeba multiplication induces chemotaxis and biofilm colonization and formation for *Legionella*. *PLoS One* **8**: e77875.
- Böck, D., Hüsler, D., Steiner, B., Medeiros, J.M., Welin, A., Ramomska, K.A., *et al.* (2021) The polar *Legionella* Icm/Dot T4SS establishes distinct contact sites with the pathogen vacuole membrane. *mBio* **12**: e02180-21.
- Bonn, F., Bartel, J., Buttner, K., Hecker, M., Otto, A., and Becher, D. (2014) Picking vanished proteins from the void: how to collect and ship/share extremely dilute proteins in a reproducible and highly efficient manner. *Anal Chem* **86**: 7421–7427.
- Carlson, H.K., Vance, R.E., and Marletta, M.A. (2010) H-NOX regulation of c-di-GMP metabolism and biofilm formation in *Legionella pneumophila*. *Mol Microbiol* **77**: 930–942.
- Chang, B., Kura, F., Amemura-Maekawa, J., Koizumi, N., and Watanabe, H. (2005) Identification of a novel adhesion molecule involved in the virulence of *Legionella pneumophila*. *Infect Immun* **73**: 4272–4280.
- Cirillo, S.L., Bermudez, L.E., El-Etr, S.H., Duhamel, G.E., and Cirillo, J.D. (2001) *Legionella pneumophila* entry gene *rtxA* is involved in virulence. *Infect Immun* **69**: 508–517.
- Davey, M.E., and O'Toole, G.A. (2000) Microbial biofilms: from ecology to molecular genetics. *Microbiol Mol Biol Rev* **64**: 847–867.
- De Buck, E., Maes, L., Meyen, E., Van Mellaert, L., Geukens, N., Anne, J., and Lammertyn, E. (2005) *Legionella pneumophila* Philadelphia-1 *tatB* and *tatC* affect intracellular replication and biofilm formation. *Biochem Biophys Res Commun* **331**: 1413–1420.
- de Felipe, K.S., Glover, R.T., Charpentier, X., Anderson, O. R., Reyes, M., Pericone, C.D., and Shuman, H.A. (2008) *Legionella* eukaryotic-like type IV substrates interfere with organelle trafficking. *PLoS Pathog* **4**: e1000117.
- Declerck, P. (2010) Biofilms: the environmental playground of *Legionella pneumophila*. *Environ Microbiol* **12**: 557–566.
- Declerck, P., Behets, J., Margineanu, A., van Hoef, V., De Keersmaecker, B., and Ollevier, F. (2009) Replication of *Legionella pneumophila* in biofilms of water distribution pipes. *Microbiol Res* **164**: 593–603.
- Declerck, P., Behets, J., van Hoef, V., and Ollevier, F. (2007) Replication of *Legionella pneumophila* in floating biofilms. *Curr Microbiol* **55**: 435–440.
- Delgado, M.G., Rivera, C.A., and Lennon-Dumenil, A.M. (2022) Macropinocytosis and cell migration: don't drink and drive. *Subcell Biochem* **98**: 85–102.
- Dietrich, C., Heuner, K., Brand, B.C., Hacker, J., and Steinert, M. (2001) Flagellum of *Legionella pneumophila* positively affects the early phase of infection of eukaryotic host cells. *Infect Immun* **69**: 2116–2122.
- Doyscher, D., Fieseler, L., Dons, L., Loessner, M.J., and Schuppler, M. (2013) *Acanthamoeba* feature a unique backpacking strategy to trap and feed on *Listeria monocytogenes* and other motile bacteria. *Environ Microbiol* **15**: 433–446.
- Duncan, C., Prashar, A., So, J., Tang, P., Low, D.E., Terebiznik, M., and Guyard, C. (2011) Lcl of *Legionella pneumophila* is an immunogenic GAG binding adhesin that promotes interactions with lung epithelial cells and plays a crucial role in biofilm formation. *Infect Immun* **79**: 2168–2181.
- Feeley, J.C., Gibson, R.J., Gorman, G.W., Langford, N.C., Rasheed, J.K., Mackel, D.C., and Baine, W.B. (1979) Charcoal-yeast extract agar: primary isolation medium for *Legionella pneumophila*. *J Clin Microbiol* **10**: 437–441.
- Fields, B.S. (1996) The molecular ecology of *Legionellae*. *Trends Microbiol* **4**: 286–290.
- Fields, B.S., Benson, R.F., and Besser, R.E. (2002) *Legionella* and Legionnaires' disease: 25 years of investigation. *Clin Microbiol Rev* **15**: 506–526.
- Finsel, I., and Hilbi, H. (2015) Formation of a pathogen vacuole according to *Legionella pneumophila*: how to kill one bird with many stones. *Cell Microbiol* **17**: 935–950.
- Ghosal, D., Jeong, K.C., Chang, Y.W., Gyore, J., Teng, L., Gardner, A., *et al.* (2019) Molecular architecture, polar targeting and biogenesis of the *Legionella* Dot/Icm T4SS. *Nat Microbiol* **4**: 1173–1182.

- Haiko, J., and Westerlund-Wikstrom, B. (2013) The role of the bacterial flagellum in adhesion and virulence. *Biology* **2**: 1242–1267.
- Hilbi, H., Hoffmann, C., and Harrison, C.F. (2011) *Legionella* spp. outdoors: colonization, communication and persistence. *Environ Microbiol Rep* **3**: 286–296.
- Hilbi, H., Segal, G., and Shuman, H.A. (2001) Icm/Dot-dependent upregulation of phagocytosis by *Legionella pneumophila*. *Mol Microbiol* **42**: 603–617.
- Hindré, T., Brüggemann, H., Buchrieser, C., and Héchard, Y. (2008) Transcriptional profiling of *Legionella pneumophila* biofilm cells and the influence of iron on biofilm formation. *Microbiology* **154**: 30–41.
- Hochstrasser, R., and Hilbi, H. (2017) Intra-species and inter-kingdom signaling of *Legionella pneumophila*. *Front Microbiol* **8**: 79.
- Hochstrasser, R., and Hilbi, H. (2019) Migration of *Acanthamoeba castellanii* through *Legionella* biofilms. *Methods Mol Biol* **1921**: 79–89.
- Hochstrasser, R., and Hilbi, H. (2020) *Legionella* quorum sensing meets cyclic-di-GMP signaling. *Curr Opin Microbiol* **55**: 9–16.
- Hochstrasser, R., and Hilbi, H. (2022) The *Legionella* Lqs-LvbR regulatory network controls temperature-dependent growth onset and bacterial cell density. *Appl Environ Microbiol* **88**: e0237021.
- Hochstrasser, R., Hutter, C.A.J., Arnold, F.M., Barlocher, K., Seeger, M.A., and Hilbi, H. (2020) The structure of the *Legionella* response regulator LqsR reveals amino acids critical for phosphorylation and dimerization. *Mol Microbiol* **113**: 1070–1084.
- Hochstrasser, R., Kessler, A., Sahr, T., Simon, S., Schell, U., Gomez-Valero, L., et al. (2019) The pleiotropic *Legionella* transcription factor LvbR links the Lqs and c-di-GMP regulatory networks to control biofilm architecture and virulence. *Environ Microbiol* **21**: 1035–1053.
- Hoffmann, C., Harrison, C.F., and Hilbi, H. (2014) The natural alternative: protozoa as cellular models for *Legionella* infection. *Cell Microbiol* **16**: 15–26.
- Horwitz, M.A. (1983) Formation of a novel phagosome by the Legionnaires' disease bacterium (*Legionella pneumophila*) in human monocytes. *J Exp Med* **158**: 1319–1331.
- Hubber, A., and Roy, C.R. (2010) Modulation of host cell function by *Legionella pneumophila* type IV effectors. *Annu Rev Cell Dev Biol* **26**: 261–283.
- Huws, S.A., McBain, A.J., and Gilbert, P. (2005) Protozoan grazing and its impact upon population dynamics in biofilm communities. *J Appl Microbiol* **98**: 238–244.
- Isberg, R.R., O'Connor, T.J., and Heidtman, M. (2009) The *Legionella pneumophila* replication vacuole: making a cosy niche inside host cells. *Nat Rev Microbiol* **7**: 13–24.
- Kessler, A., Schell, U., Sahr, T., Tieden, A., Harrison, C., Buchrieser, C., and Hilbi, H. (2013) The *Legionella pneumophila* orphan sensor kinase LqsT regulates competence and pathogen-host interactions as a component of the LAI-1 circuit. *Environ Microbiol* **15**: 646–662.
- Kubori, T., and Nagai, H. (2016) The type IVB secretion system: an enigmatic chimera. *Curr Opin Microbiol* **29**: 22–29.
- Kuiper, M.W., Wullings, B.A., Akkermans, A.D., Beumer, R. R., and van der Kooij, D. (2004) Intracellular proliferation of *Legionella pneumophila* in *Hartmannella vermiformis* in aquatic biofilms grown on plasticized polyvinyl chloride. *Appl Environ Microbiol* **70**: 6826–6833.
- Lau, H.Y., and Ashbolt, N.J. (2009) The role of biofilms and protozoa in *Legionella* pathogenesis: implications for drinking water. *J Appl Microbiol* **107**: 368–378.
- Lucas, C.E., Brown, E., and Fields, B.S. (2006) Type IV pili and type II secretion play a limited role in *Legionella pneumophila* biofilm colonization and retention. *Microbiology* **152**: 3569–3573.
- Maass, S., Sievers, S., Zuhlke, D., Kuzinski, J., Sappa, P.K., Muntel, J., et al. (2011) Efficient, global-scale quantification of absolute protein amounts by integration of targeted mass spectrometry and two-dimensional gel-based proteomics. *Anal Chem* **83**: 2677–2684.
- Mallegol, J., Duncan, C., Prashar, A., So, J., Low, D.E., Terebeznik, M., and Guyard, C. (2012) Essential roles and regulation of the *Legionella pneumophila* collagen-like adhesin during biofilm formation. *PLoS One* **7**: e46462.
- Mampel, J., Spirig, T., Weber, S.S., Haagensen, J.A.J., Molin, S., and Hilbi, H. (2006) Planktonic replication is essential for biofilm formation by *Legionella pneumophila* in a complex medium under static and dynamic flow conditions. *Appl Environ Microbiol* **72**: 2885–2895.
- Manske, C., Schell, U., and Hilbi, H. (2016) Metabolism of myo-inositol by *Legionella pneumophila* promotes infection of amoebae and macrophages. *Appl Environ Microbiol* **82**: 5000–5014.
- Matz, C., and Kjelleberg, S. (2005) Off the hook – how bacteria survive protozoan grazing. *Trends Microbiol* **13**: 302–307.
- Moffat, J.F., and Tompkins, L.S. (1992) A quantitative model of intracellular growth of *Legionella pneumophila* in *Acanthamoeba castellanii*. *Infect Immun* **60**: 296–301.
- Murga, R., Forster, T.S., Brown, E., Pruckler, J.M., Fields, B. S., and Donlan, R.M. (2001) Role of biofilms in the survival of *Legionella pneumophila* in a model potable-water system. *Microbiology* **147**: 3121–3126.
- Nagai, H., Kagan, J.C., Zhu, X., Kahn, R.A., and Roy, C.R. (2002) A bacterial guanine nucleotide exchange factor activates ARF on *Legionella* phagosomes. *Science* **295**: 679–682.
- Neunuebel, M.R., Chen, Y., Gaspar, A.H., Backlund, P.S., Jr., Yergey, A., and Machner, M.P. (2011) De-AMPylation of the small GTPase Rab1 by the pathogen *Legionella pneumophila*. *Science* **333**: 453–456.
- Newton, H.J., Ang, D.K., van Driel, I.R., and Hartland, E.L. (2010) Molecular pathogenesis of infections caused by *Legionella pneumophila*. *Clin Microbiol Rev* **23**: 274–298.
- Pécastaings, S., Allombert, J., Lajoie, B., Doublet, P., Roques, C., and Vianney, A. (2016) New insights into *Legionella pneumophila* biofilm regulation by c-di-GMP signaling. *Biofouling* **32**: 935–948.
- Pécastaings, S., Berge, M., Dubourg, K.M., and Roques, C. (2010) Sessile *Legionella pneumophila* is able to grow on surfaces and generate structured monospecies biofilms. *Biofouling* **26**: 809–819.
- Perez-Riverol, Y., Csordas, A., Bai, J., Bernal-Llinares, M., Hewapathirana, S., Kundu, D.J., et al. (2019) The PRIDE database and related tools and resources in 2019: improving support for quantification data. *Nucleic Acids Res* **47**: D442–D450.

- Personnic, N., Bärlocher, K., Finsel, I., and Hilbi, H. (2016) Subversion of retrograde trafficking by translocated pathogen effectors. *Trends Microbiol* **24**: 450–462.
- Personnic, N., Striednig, B., and Hilbi, H. (2018) *Legionella* quorum sensing and its role in pathogen-host interactions. *Curr Opin Microbiol* **41**: 29–35.
- Personnic, N., Striednig, B., and Hilbi, H. (2021) Quorum sensing controls persistence, resuscitation, and virulence of *Legionella* subpopulations in biofilms. *ISME J* **15**: 196–210.
- Personnic, N., Striednig, B., Lezan, E., Manske, C., Welin, A., Schmidt, A., and Hilbi, H. (2019) Quorum sensing modulates the formation of virulent *Legionella* persists within infected cells. *Nat Commun* **10**: 5216.
- Petrova, O.E., and Sauer, K. (2012) Sticky situations: key components that control bacterial surface attachment. *J Bacteriol* **194**: 2413–2425.
- Qiu, J., and Luo, Z.Q. (2017) *Legionella* and *Coxiella* effectors: strength in diversity and activity. *Nat Rev Microbiol* **15**: 591–605.
- Qiu, J., Sheedlo, M.J., Yu, K., Tan, Y., Nakayasu, E.S., Das, C., et al. (2016) Ubiquitination independent of E1 and E2 enzymes by bacterial effectors. *Nature* **533**: 120–124.
- Ronn, R., McCaig, A.E., Griffiths, B.S., and Prosser, J.I. (2002) Impact of protozoan grazing on bacterial community structure in soil microcosms. *Appl Environ Microbiol* **68**: 6094–6105.
- Rothmeier, E., Pfaffinger, G., Hoffmann, C., Harrison, C.F., Grabmayr, H., Repnik, U., et al. (2013) Activation of Ran GTPase by a *Legionella* effector promotes microtubule polymerization, pathogen vacuole motility and infection. *PLoS Pathog* **9**: e1003598.
- Sadosky, A.B., Wiater, L.A., and Shuman, H.A. (1993) Identification of *Legionella pneumophila* genes required for growth within and killing of human macrophages. *Infect Immun* **61**: 5361–5373.
- Schell, U., Kessler, A., and Hilbi, H. (2014) Phosphorylation signalling through the *Legionella* quorum sensing histidine kinases LqsS and LqsT converges on the response regulator LqsR. *Mol Microbiol* **92**: 1039–1055.
- Schell, U., Simon, S., Sahr, T., Hager, D., Albers, M.F., Kessler, A., et al. (2016) The α -hydroxyketone LAI-1 regulates motility, Lqs-dependent phosphorylation signalling and gene expression of *Legionella pneumophila*. *Mol Microbiol* **99**: 778–793.
- Segal, G., Russo, J.J., and Shuman, H.A. (1999) Relationships between a new type IV secretion system and the *icm/dot* virulence system of *Legionella pneumophila*. *Mol Microbiol* **34**: 799–809.
- Segal, G., and Shuman, H.A. (1998) Intracellular multiplication and human macrophage killing by *Legionella pneumophila* are inhibited by conjugal components of IncQ plasmid RSF1010. *Mol Microbiol* **30**: 197–208.
- Segal, G., and Shuman, H.A. (1999) *Legionella pneumophila* utilizes the same genes to multiply within *Acanthamoeba castellanii* and human macrophages. *Infect Immun* **67**: 2117–2124.
- Simon, S., Schell, U., Heuer, N., Hager, D., Albers, M.F., Matthias, J., et al. (2015) Inter-kingdom signaling by the *Legionella* quorum sensing molecule LAI-1 modulates cell migration through an IQGAP1-Cdc42-ARHGEF9-dependent pathway. *PLoS Pathog* **11**: e1005307.
- Simon, S., Wagner, M.A., Rothmeier, E., Müller-Taubenberger, A., and Hilbi, H. (2014) Icm/Dot-dependent inhibition of phagocyte migration by *Legionella* is antagonized by a translocated Ran GTPase activator. *Cell Microbiol* **16**: 977–992.
- Spirig, T., Tiaden, A., Kiefer, P., Buchrieser, C., Vorholt, J.A., and Hilbi, H. (2008) The *Legionella* autoinducer synthase LqsA produces an α -hydroxyketone signaling molecule. *J Biol Chem* **283**: 18113–18123.
- Sreelatha, A., Nolan, C., Park, B.C., Pawlowski, K., Tomchick, D.R., and Tagliabracci, V.S. (2020) A *Legionella* effector kinase is activated by host inositol hexakisphosphate. *J Biol Chem* **295**: 6214–6224.
- Steiner, B., Swart, A.L., Welin, A., Weber, S., Personnic, N., Kaech, A., et al. (2017) ER remodeling by the large GTPase atlastin promotes vacuolar growth of *Legionella pneumophila*. *EMBO Rep* **18**: 1817–1836.
- Steiner, B., Weber, S., and Hilbi, H. (2018) Formation of the *Legionella*-containing vacuole: phosphoinositide conversion, GTPase modulation and ER dynamics. *Int J Med Microbiol* **308**: 49–57.
- Stewart, C.R., Muthye, V., and Cianciotto, N.P. (2012) *Legionella pneumophila* persists within biofilms formed by *Klebsiella pneumoniae*, *Flavobacterium* sp., and *Pseudomonas fluorescens* under dynamic flow conditions. *PLoS One* **7**: e50560.
- Striednig, B., Lanner, U., Niggli, S., Katic, A., Vormittag, S., Brülisauer, S., et al. (2021) Quorum sensing governs a transmissible *Legionella* subpopulation at the pathogen vacuole periphery. *EMBO Rep* **22**: e52972.
- Swart, A.L., Gomez-Valero, L., Buchrieser, C., and Hilbi, H. (2020a) Evolution and function of bacterial RCC1 repeat effectors. *Cell Microbiol* **22**: e13246.
- Swart, A.L., Harrison, C.F., Eichinger, L., Steinert, M., and Hilbi, H. (2018) *Acanthamoeba* and *Dictyostelium* as cellular models for *Legionella* infection. *Front Cell Infect Microbiol* **8**: 61.
- Swart, A.L., Steiner, B., Gomez-Valero, L., Schutz, S., Hannemann, M., Janning, P., et al. (2020b) Divergent evolution of *Legionella* RCC1 repeat effectors defines the range of Ran GTPase cycle targets. *mBio* **11**: e00405-20.
- Tan, Y., and Luo, Z.Q. (2011) *Legionella pneumophila* SidD is a deAMPylase that modifies Rab1. *Nature* **475**: 506–509.
- Tiaden, A., and Hilbi, H. (2012) α -Hydroxyketone synthesis and sensing by *Legionella* and *Vibrio*. *Sensors* **12**: 2899–2919.
- Tiaden, A., Spirig, T., Carranza, P., Brüggemann, H., Riedel, K., Eberl, L., et al. (2008) Synergistic contribution of the *Legionella pneumophila* lqs genes to pathogen-host interactions. *J Bacteriol* **190**: 7532–7547.
- Tiaden, A., Spirig, T., and Hilbi, H. (2010a) Bacterial gene regulation by α -hydroxyketone signaling. *Trends Microbiol* **18**: 288–297.
- Tiaden, A., Spirig, T., Sahr, T., Wälti, M.A., Boucke, K., Buchrieser, C., and Hilbi, H. (2010b) The autoinducer synthase LqsA and putative sensor kinase LqsS regulate phagocyte interactions, extracellular filaments and a genomic island of *Legionella pneumophila*. *Environ Microbiol* **12**: 1243–1259.

- Tiaden, A., Spirig, T., Weber, S.S., Brüggemann, H., Bosshard, R., Buchrieser, C., and Hilbi, H. (2007) The *Legionella pneumophila* response regulator LqsR promotes host cell interactions as an element of the virulence regulatory network controlled by RpoS and LetA. *Cell Microbiol* **9**: 2903–2920.
- Vandersmissen, L., De Buck, E., Saels, V., Coil, D.A., and Anne, J. (2010) A *Legionella pneumophila* collagen-like protein encoded by a gene with a variable number of tandem repeats is involved in the adherence and invasion of host cells. *FEMS Microbiol Lett* **306**: 168–176.
- Veltman, D.M. (2015) Drink or drive: competition between macropinocytosis and cell migration. *Biochem Soc Trans* **43**: 129–132.
- Vizcaino, J.A., Csordas, A., del-Toro, N., Dianes, J.A., Griss, J., Lavidas, I., et al. (2016) 2016 update of the PRIDE database and its related tools. *Nucleic Acids Res* **44**: D447–D456.
- Weber, S.S., Joller, N., Kuntzel, A.B., Spörri, R., Tchang, V. S., Scandella, E., et al. (2012) Identification of protective B cell antigens of *Legionella pneumophila*. *J Immunol* **189**: 841–849.
- Weber, S.S., Ragaz, C., Reus, K., Nyfeler, Y., and Hilbi, H. (2006) *Legionella pneumophila* exploits PI(4)P to anchor secreted effector proteins to the replicative vacuole. *PLoS Pathog* **2**: e46.

Supporting Information

Additional Supporting Information may be found in the online version of this article at the publisher's web-site:

Fig. S1. Heat map of proteins depleted or enriched in $\Delta lvbR$ and $\Delta lqsR$ biofilms compared to JR32.

Comparative proteomics was performed with biofilms formed by *L. pneumophila* JR32, $\Delta lvbR$ or $\Delta lqsR$. In the heat map all proteins are shown that are depleted or enriched in mutant biofilms (for details see Materials and Methods). Biofilm bacteria were harvested by centrifugation and supernatants (designated 's', extracellular) and cell pellets (designated 'p', intracellular) were analysed separately. The proteins are listed by ascending Lpg numbers. The colour code indicates the level of regulation: the darker the colour the stronger the corresponding gene is regulated (red: depleted proteins, max. 2^{-5} ; blue: accumulated proteins, max. $2^{7.4}$). Boxes highlight regions of interest, which are further discussed. 'NaN': not a number.

Fig. S2. Biofilm formation and quantification of *L. pneumophila* strains.

(A) Biofilms were initiated with exponential phase *L. pneumophila* $\Delta lqsS$, $\Delta lqsT$ or $\Delta lqsS-\Delta lqsT$ mutant strains harbouring pNT28 (constitutive production of GFP) in AYE medium within ibiTreat microscopy dishes. Biofilms were grown at 25°C without mechanical disturbance and confocal microscopy images of biofilm architecture were acquired at 4 μm above dish bottom after 1, 2, 3 and 6 days of growth. The images shown are representative of at least two independent experiments. Scale bars, 30 μm . (B, C) Quantification of *L. pneumophila* biofilms grown for 6 days. (B) Pseudocolour graph (GFP intensity vs. FSC) depicting the gate for GFP-producing *L. pneumophila* (identified by

fluorescence) and the beads population (identified by SSC vs. FSC). (C) Means and standard deviation (bacteria/ml) of biological triplicates from 100'000 events of each biofilm suspension (differences between wild-type and mutant *L. pneumophila* are statistically not significant).

Fig. S3. Surface adherence of biofilms formed by *L. pneumophila* JR32 and mutant strains.

Biofilms were initiated with exponential phase *L. pneumophila* JR32, $\Delta lvbR$, $\Delta lqsR$, $\Delta lqsA$, $\Delta lqsS$, $\Delta lqsT$, $\Delta lqsS-\Delta lqsT$, $\Delta flaA$ or $\Delta icmT$ mutant strains harbouring pNT28 (constitutive production of GFP) in AYE medium within ibiTreat microscopy dishes. Biofilms were grown at 25°C without mechanical disturbance and confocal microscopy images of biofilm attachments were acquired at the dish bottom (0 μm) after 1, 2, 3 and 6 days of growth. The images shown are representative of at least two independent experiments. Scale bars, 10 μm .

Fig. S4. *L. pneumophila* cluster formation on *A. castellanii* in JR32 or mutant strain biofilms.

Biofilms of (A) *L. pneumophila* JR32, $\Delta lvbR$, $\Delta lqsR$, $\Delta lqsA$, $\Delta flaA$ or $\Delta icmT$ mutant strains harbouring pNT28 (constitutive production of GFP), or (B, C) strain JR32 harbouring pNT28 were grown for 6 days in AYE medium at 25°C, and *A. castellanii* was added to preformed biofilms. Bacterial adherence and cluster formation were monitored by confocal microscopy (A, B) ca. 4 μm above or (C) at the dish bottom ("clusters": arrow heads, "trails": arrows). (D, E) Biofilms of *L. pneumophila* JR32 or $\Delta flaA$ mutant strains constitutively producing GFP (pNT28) or GFP and FlaA under control of its promoter ($\Delta flaA/+flaA$, pSB001) were grown for 6 days in AYE medium at 25°C, and *A. castellanii* was added to preformed biofilms. Confocal microscopy images of (D) overview and (E) zoom-in of *L. pneumophila* adherence and cluster formation on amoebae. The images shown are representative of three independent experiments. Scale bars, 30 μm .

Fig. S5. Quantification of amoeba-associated *L. pneumophila* clusters by flow cytometry.

Quantification by flow cytometry (forward scatter area, FSC-A, vs. fluorescence intensity) using FlowJo software of (A) *L. pneumophila* strain JR32 or *A. castellanii*, (B) amoebae-associated or non-associated, GFP-positive *L. pneumophila* JR32, $\Delta lvbR$, $\Delta lqsR$, $\Delta lqsA$, $\Delta flaA$ or $\Delta icmT$ harbouring pNT28 (protocol #1, see Material and Methods), or (C) non-associated, GFP-positive *L. pneumophila* JR32 harbouring promoter expression reporters (P_{flaA} , P_{6SRNA} , P_{sidC} , P_{ralF} , or P_{csrA}) (protocol #2, see Material and Methods).

Fig. S6. Competition of mCherry-producing *L. pneumophila* JR32 and GFP-producing mutants for cluster formation on amoebae.

Biofilm formation was initiated with a 1:1 ratio of exponential phase mCherry-producing *L. pneumophila* JR32 (pNP102) and GFP-producing JR32 or mutant strains (pNT28). Biofilms were grown in AYE medium within ibiTreat microscopy dishes at 25°C for 6 days. *A. castellanii* were added to preformed biofilms, and amoebae with adherent bacterial clusters were monitored by confocal microscopy above dish bottom. The images shown are representative of at least two independent experiments. Scale bars, 30 μm .

Fig. S7. Gene expression kinetics of *L. pneumophila* JR32 in AYE medium using single promoter reporters.

L. pneumophila JR32 harbouring (A) P_{flaA} -*gfp* (pCM009), (B) P_{6SRNA} -*gfp* (pRH049), (C) P_{sidC} -*gfp* (pRH035), (D) P_{raiF} -*gfp* (pRH032) or (E) P_{csrA} -*gfp* (pRH031) reporter constructs were grown at 37°C in AYE medium in microplates while orbitally shaking. GFP fluorescence (relative fluorescence units, RFU) at a gain of 50 and optical density at 600 nm (OD_{600}) were monitored over time using a microplate reader. The kinetics of the GFP fluorescence or OD_{600} values are shown and depicted by the left or right y-axis respectively. The data are means and standard deviations of technical triplicates and representative of three independent measurements.

Fig. S8. Gene expression kinetics of *L. pneumophila* JR32 in AYE medium and in amoeba-adherent bacteria in biofilms using dual promoter reporters.

L. pneumophila JR32 harbouring (A) P_{flaA} -*gfp* (pSN7) or (B) P_{6SRNA} -*gfp* (pSN25) reporter constructs were grown at 37°C in AYE medium within microplates while orbitally shaking. GFP fluorescence (relative fluorescence units, RFU) at a gain of 50 and optical density at 600 nm (OD_{600}) were monitored over time using a microplate reader. The kinetics of the

GFP fluorescence (left y-axis) or OD_{600} (right y-axis) values are shown. The data are means and standard deviations of technical triplicates and representative of three independent measurements. (C, D) Biofilms of *L. pneumophila* JR32, $\Delta lvbR$ or $\Delta lqsR$ harbouring dual reporter plasmids expressing P_{tac} -*mcherry* (constitutive) and P_{flaA} -*gfp* (pSN7) or P_{6SRNA} -*gfp* (pSN25) were grown in AYE medium for 6 days. *A. castellanii* was added to preformed biofilms, and confocal microscopy images of amoebae with adherent bacterial clusters were acquired close to the bottom of microscopy dishes. The images shown are representative of 2–3 independent experiments. Scale bars, 30 μ m.

Table S1. Oligonucleotides used in this study.

Movie S1. Motility of *L. pneumophila* JR32.

Movie S2. Motility of *L. pneumophila* $\Delta lvbR$.

Movie S3. Motility of *L. pneumophila* $\Delta lqsR$.

Movie S4. *A. castellanii* migrating through JR32 biofilm.

Movie S5. *A. castellanii* migrating through $\Delta lvbR$ biofilm.

Movie S6. *A. castellanii* migrating through $\Delta lqsR$ biofilm.

Movie S7. *A. castellanii* migrating through $\Delta lqsA$ biofilm.

Movie S8. *A. castellanii* migrating through $\Delta flaA$ biofilm.

Movie S9. *A. castellanii* migrating through $\Delta icmT$ biofilm.